p–ϕ femtoscopic correlation analysis using a dynamical model

SOPHIA U

SOPHIA HADRON PHYSICS GROUP

Kenshi Kuroki (Sophia University)

In collaboration with

Tetsufumi Hirano (Sophia University)

SQM2024

The 21st International Conference on Strangeness in Quark Matter, Strasbourg, France, June 5, 2024

Hadron correlations in nuclear collisions

→ **Useful for studying hadron interactions**

Correlation Function (CF) at Pair Rest Frame ($\boldsymbol{P} = 0$)

$$C(\boldsymbol{q}) := \frac{N_{\mathrm{pair}}(\boldsymbol{p}_a, \boldsymbol{p}_b)}{N_a(\boldsymbol{p}_a)\, N_b(\boldsymbol{p}_b)}$$

Total momentum: $\boldsymbol{P} = \boldsymbol{p}_a + \boldsymbol{p}_b$

Relative momentum: $\boldsymbol{q} = \frac{m_b \boldsymbol{p}_a - m_a \boldsymbol{p}_b}{m_a + m_b}$

Two-particle momentum dist.: $N_{\mathrm{pair}}(\boldsymbol{p}_a, \boldsymbol{p}_b)$

One-particle momentum dist.: $N_a(\boldsymbol{p}_a)$

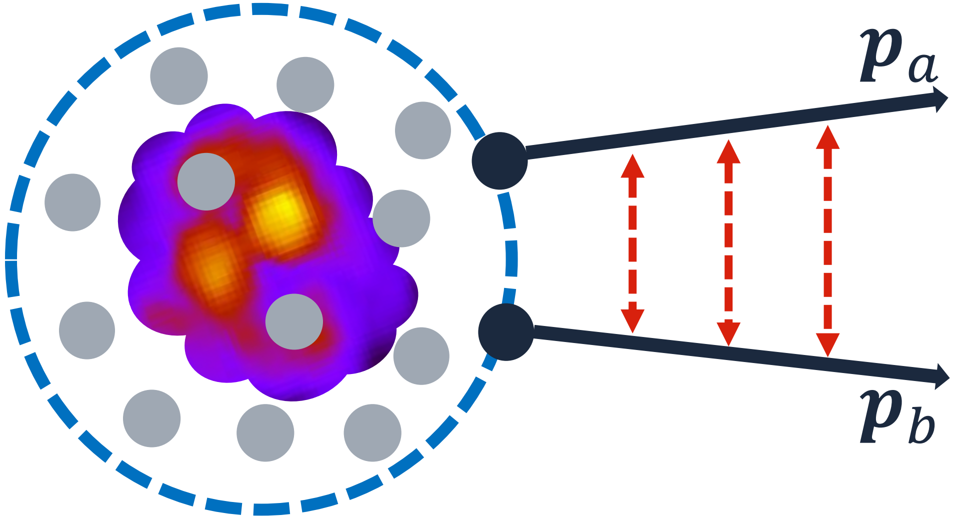

Hadron CF contains information on

- **Space-time structure of the matter**
- **Final state hadron interactions**

Koonin-Pratt (KP) formula

S. E. Koonin, PLB **70**, 43 (1977); S. Pratt, PRD **33**, 1314 (1986)

$$C(\boldsymbol{q}) = \int d^3r \; S(\boldsymbol{q};\boldsymbol{r}) \; |\varphi(\boldsymbol{q};\boldsymbol{r})|^2$$

CF ⇦ **Source Func.** & **Relative w.f.**

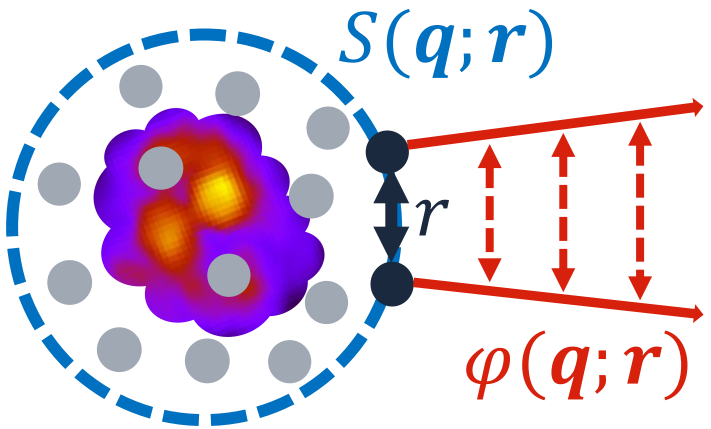

Koonin-Pratt (KP) formula

S. E. Koonin, PLB **70**, 43 (1977); S. Pratt, PRD **33**, 1314 (1986)

$$C(\boldsymbol{q}) = \int d^3r \; S(\boldsymbol{q};\boldsymbol{r}) \; |\varphi(\boldsymbol{q};\boldsymbol{r})|^2$$

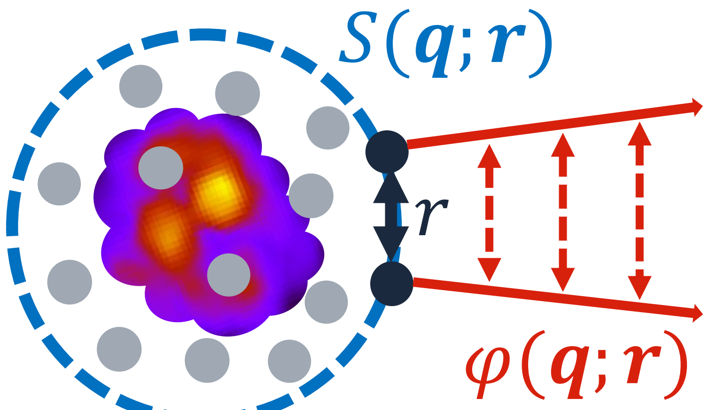

CF ⇐ **Source Func.** & **Relative w.f.**

From **measured** correlation function

- **Input**: hadron interaction → **Output**: source function
- **Input**: source function → **Output**: hadron interaction

Koonin-Pratt (KP) formula

S. E. Koonin, PLB **70**, 43 (1977); S. Pratt, PRD **33**, 1314 (1986)

$$C(\boldsymbol{q}) = \int d^3r \ S(\boldsymbol{q};\boldsymbol{r}) \ |\varphi(\boldsymbol{q};\boldsymbol{r})|^2$$

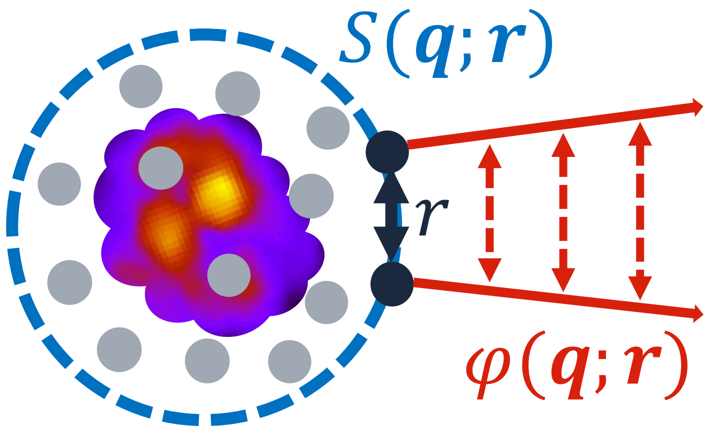

CF ⇦ **Source Func.** & **Relative w.f.**

From **measured** correlation function

- **Input**: hadron interaction → **Output**: source function
- **Input**: source function → **Output**: hadron interaction

Only s-wave scatt. with spherical SF

Weight Function

$$C(q) = 1 + \int_0^\infty dr \ 4\pi r^2 S(q;r) \ \{|\varphi_0(q;r)|^2 - [j_0(qr)]^2\}$$

Deviation of CF from 1 = How much SF “picks up” WF

p–ϕ femtoscopy

Experimental CF ALICE, PRL **127**, 172301 (2021)

High-multiplicity (0–0.17%) **p+p collisions at** $\sqrt{s} = 13$ TeV

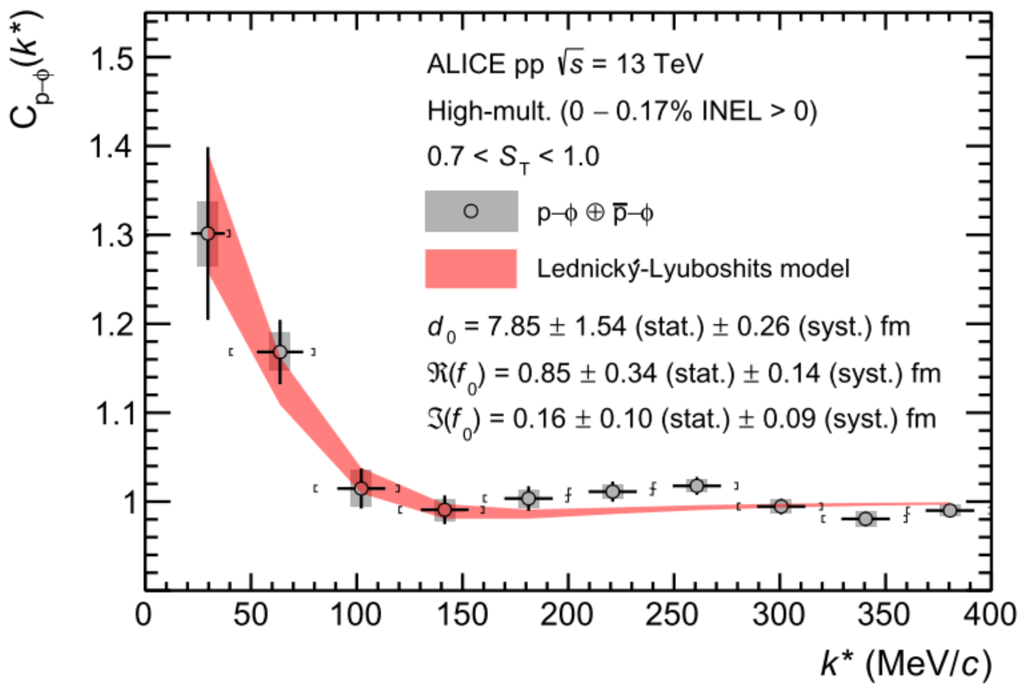

p–ϕ femtoscopy

Experimental CF
ALICE, PRL **127**, 172301 (2021)

High-multiplicity (0–0.17%) **p+p collisions at** $\sqrt{s} = 13$ TeV

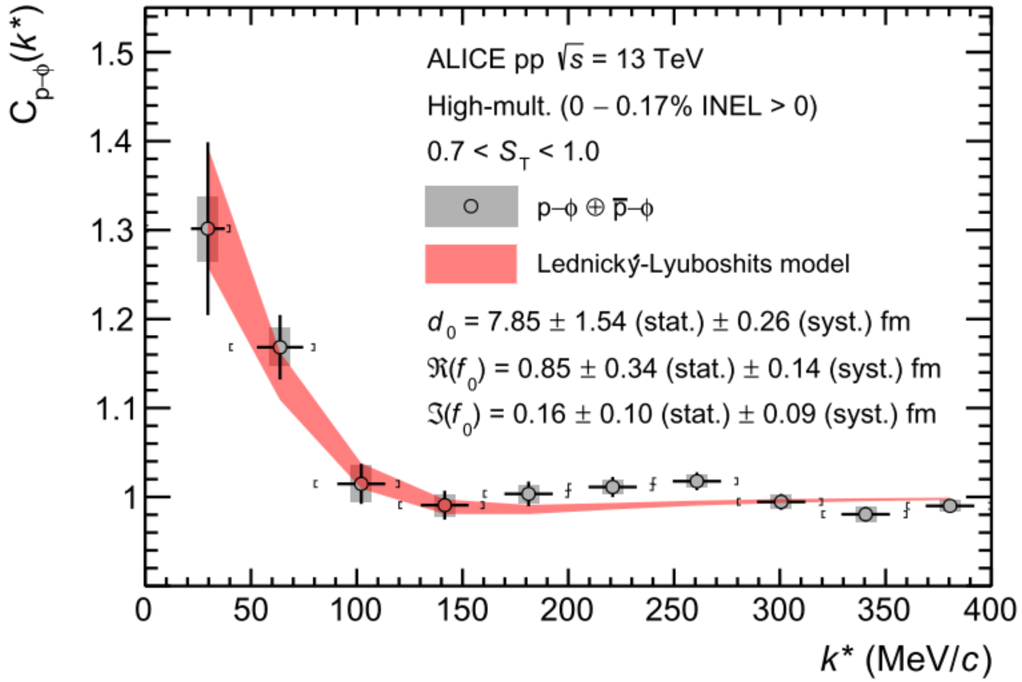

Lednický-Lyuboshits fit
R. Lednický and V. L. Lyuboshits, Yad. Fiz. **35**, 1316 (1981)

Gaussian source size: $r_0 = 1.08$ fm

Scattering length: $a_0 \cong -0.85 - 0.16i$ fm

Effective range: $r_{\mathrm{eff}} \cong 7.85$ fm

Attractive p–ϕ interaction as a spin-average

p–ϕ femtoscopy

Spin-channel-by-channel femtoscopy E. Chizzali *et al.*, PLB **848**, 138358 (2023)

Gaussian source size: $r_0 = 1.08$ fm

$^4S_{3/2}$: HAL QCD potential Y. Lyu *et al.*, PRD 106, 074507 (2022)

$a_0^{(3/2)} \cong -1.43$ fm, $r_{\mathrm{eff}}^{(3/2)} \cong 2.36$ fm

Attraction without bound states

$^2S_{1/2}$: **Parameterised potential** ← **Constrain by experimental CF**

p–ϕ femtoscopy

Spin-channel-by-channel femtoscopy

E. Chizzali *et al.*, PLB **848**, 138358 (2023)

Gaussian source size: $r_0 = 1.08$ fm

$^4S_{3/2}$: HAL QCD potential Y. Lyu *et al.*, PRD 106, 074507 (2022)

$a_0^{(3/2)} \cong -1.43$ fm, $r_{\mathrm{eff}}^{(3/2)} \cong 2.36$ fm

Attraction without bound states

$^2S_{1/2}$: **Parameterised potential** ← **Constrain by experimental CF**

$a_0^{(1/2)} \cong 1.54 - i0.00$ fm, $r_{\mathrm{eff}}^{(1/2)} \cong 0.39 + i0.00$ fm

- **Strong attraction**
- **Small effects of channel-coupling**

Indication of a p–ϕ bound state

Overview of the present study

SF should reflect the complex dynamics of nuclear collisions

This study: **Femtoscopy using SF from a dynamical model**

Overview of the present study

SF should reflect the complex dynamics of nuclear collisions

This study: **Femtoscopy using SF from a dynamical model**

p–ϕ potential

$^4S_{3/2}$: Lattice QCD $^2S_{1/2}$: **Parameterisation**

Schrödinger eq.

WF

Overview of the present study

SF should reflect the complex dynamics of nuclear collisions

This study: **Femtoscopy using SF from a dynamical model**

p–ϕ potential

$^4S_{3/2}$: Lattice QCD $^2S_{1/2}$: **Parameterisation**

Schrödinger eq.

New

SF from **a dynamical model**

WF

KP formula

New

p–ϕ CF from **a dynamical model**

Overview of the present study

SF should reflect the complex dynamics of nuclear collisions

This study: **Femtoscopy using SF from a dynamical model**

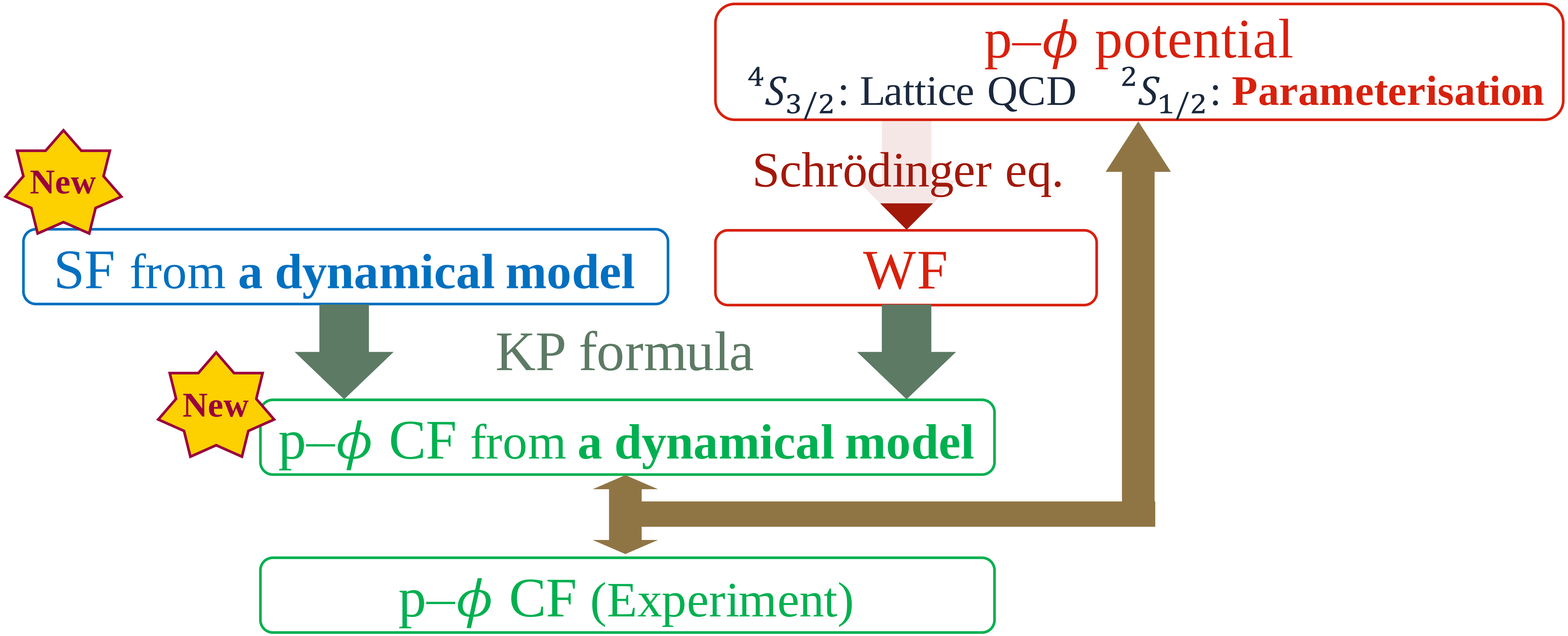

Overview of the present study

SF should reflect the complex dynamics of nuclear collisions

This study: **Femtoscopy using SF from a dynamical model**

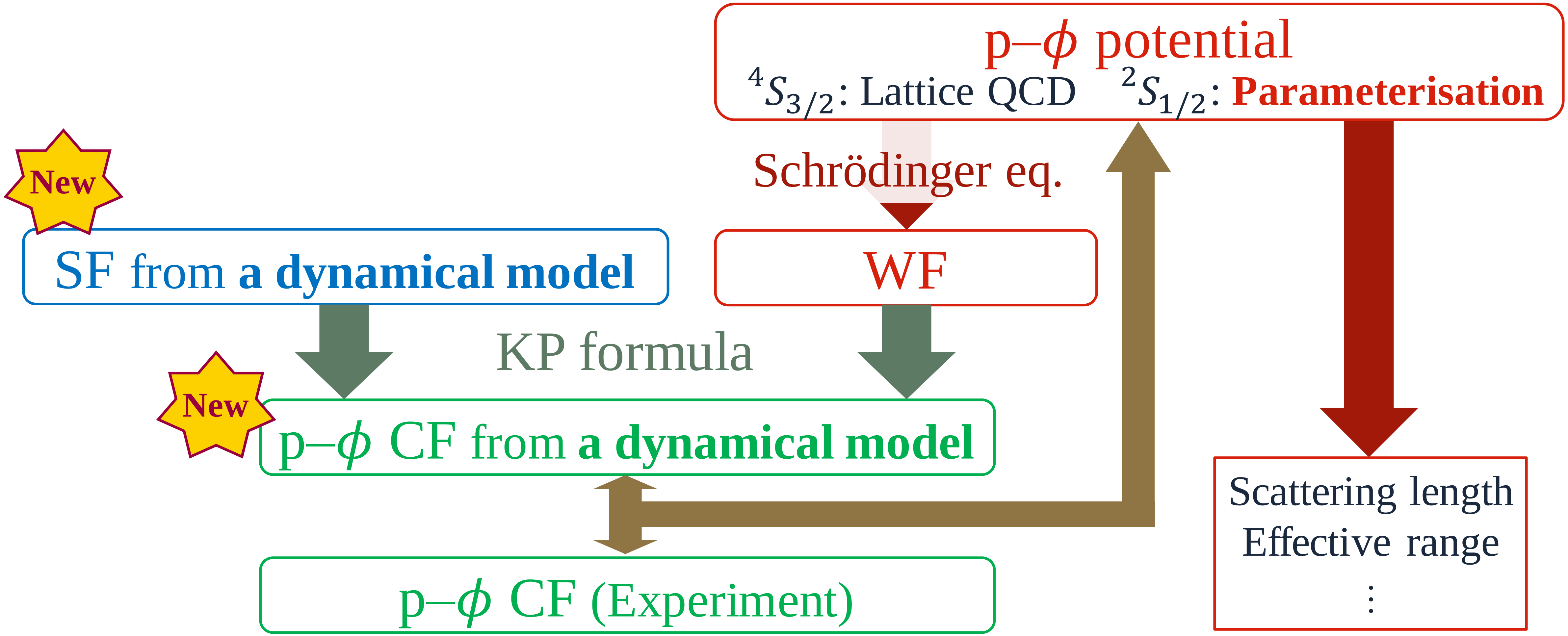

${}^4S_{3/2}$ Channel

HAL QCD potential
Y. Lyu *et al.*, PRD **106**, 074507 (2022)

Lattice QCD at nearly physical point ($m_\pi = 146.4$ MeV)

$$V^{(3/2)}(r) = \underbrace{a_1 e^{-(r/b_1)^2} + a_2 e^{-(r/b_2)^2}}_{\text{Short-range attraction}} + \underbrace{a_3 m_\pi^4 f(r;b_3) \frac{e^{-2m_\pi r}}{r^2}}_{\text{TPE}}$$

Argonne-type form factor:
$$f(r;b_3) = \left[1 - e^{-(r/b_3)^2}\right]^2$$

Parameter	Fitted value
a_1 [MeV]	-371 ± 27
b_1 [fm]	0.13 ± 0.01
a_2 [MeV]	-119 ± 39
b_2 [fm]	0.30 ± 0.05
a_3 [fm^5]	-1.62 ± 0.23
b_3 [fm]	0.63 ± 0.04

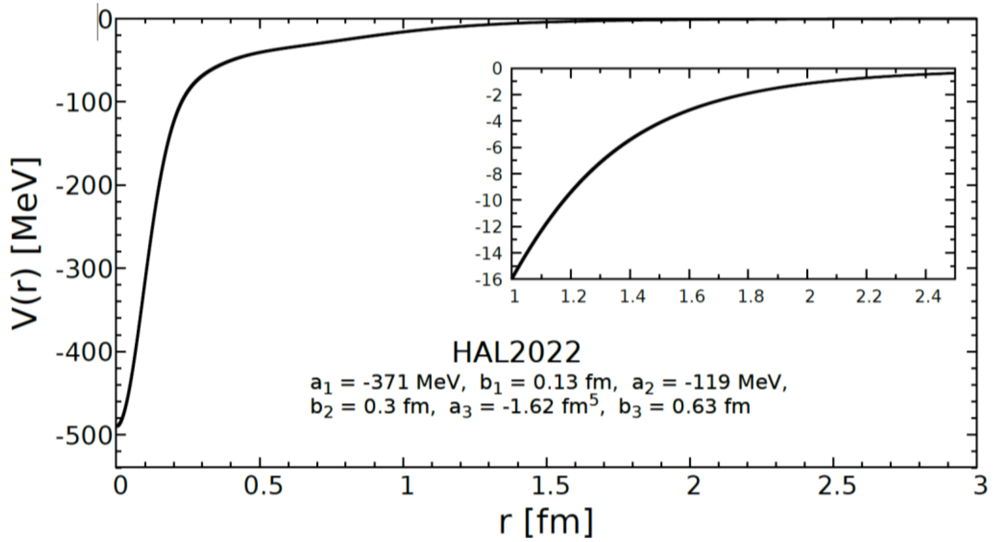

No bound state

$^4S_{3/2}$ Channel

HAL QCD potential
Y. Lyu *et al.*, PRD **106**, 074507 (2022)

Lattice QCD at nearly physical point ($m_\pi = 146.4$ MeV)

$$V^{(3/2)}(r) = \underbrace{a_1 e^{-(r/b_1)^2} + a_2 e^{-(r/b_2)^2}}_{\text{Short-range attraction}} + \underbrace{a_3 m_\pi^4 f(r;b_3)\frac{e^{-2m_\pi r}}{r^2}}_{\text{TPE}}$$

Argonne-type form factor:
$f(r;b_3) = \left[1 - e^{-(r/b_3)^2}\right]^2$

Parameter	Fitted value
a_1 [MeV]	-371 ± 27
b_1 [fm]	0.13 ± 0.01
a_2 [MeV]	-119 ± 39
b_2 [fm]	0.30 ± 0.05
a_3 [fm^5]	-1.62 ± 0.23
b_3 [fm]	0.63 ± 0.04

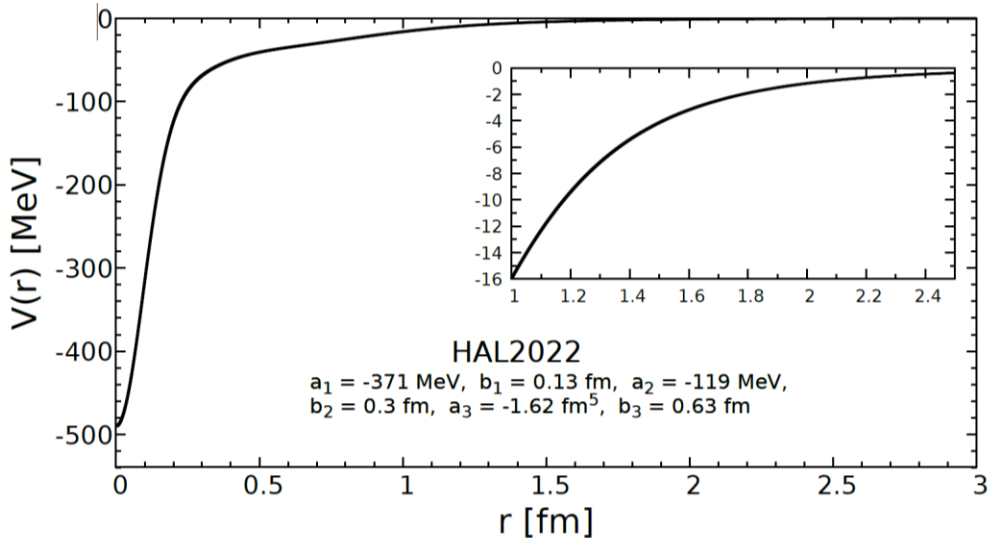

No bound state

WF: $|\varphi_0|^2 - (j_0)^2$

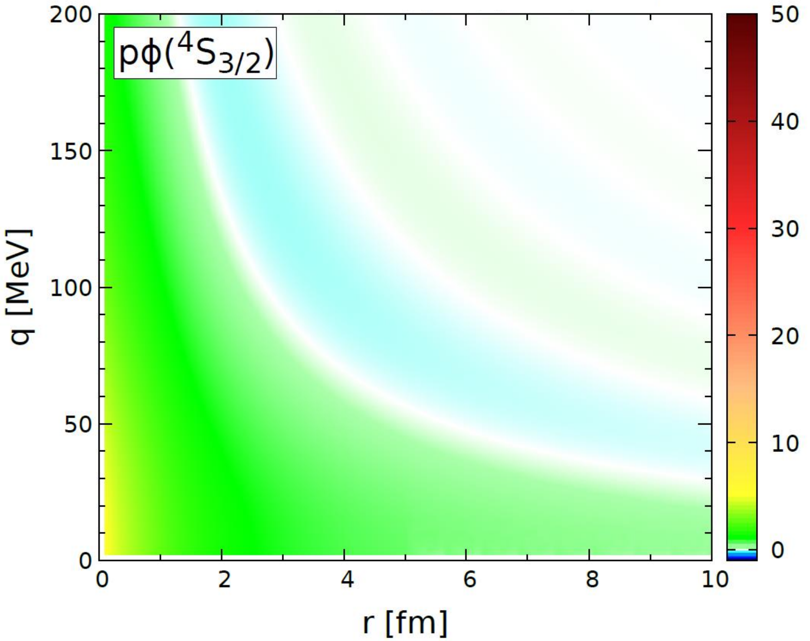

Enhancement at small ***qr***
due to attraction

$^2S_{1/2}$ Channel

Parameterised potential E. Chizzali *et al.*, PLB **848**, 138358 (2023)

Channel-couplings are neglected for simplicity

$$V^{(1/2)}(r) = \underbrace{\beta\left[a_1 e^{-(r/b_1)^2} + a_2 e^{-(r/b_2)^2}\right]}_{\text{Short-range interaction}} + \underbrace{a_3 m_\pi^4 f(r; b_3) \frac{e^{-2m_\pi r}}{r^2}}_{\text{TPE}}$$

Only one adjustable parameter

β

default: $\beta = 7$

${}^2S_{1/2}$ Channel

Only one adjustable parameter
β
default: $\beta = 7$

Parameterised potential E. Chizzali *et al.*, PLB **848**, 138358 (2023)

Channel-couplings are neglected for simplicity

$$V^{(1/2)}(r) = \underbrace{\beta\left[a_1 e^{-(r/b_1)^2} + a_2 e^{-(r/b_2)^2}\right]}_{\text{Short-range interaction}} + \underbrace{a_3 m_\pi^4 f(r;b_3)\frac{e^{-2m_\pi r}}{r^2}}_{\text{TPE}}$$

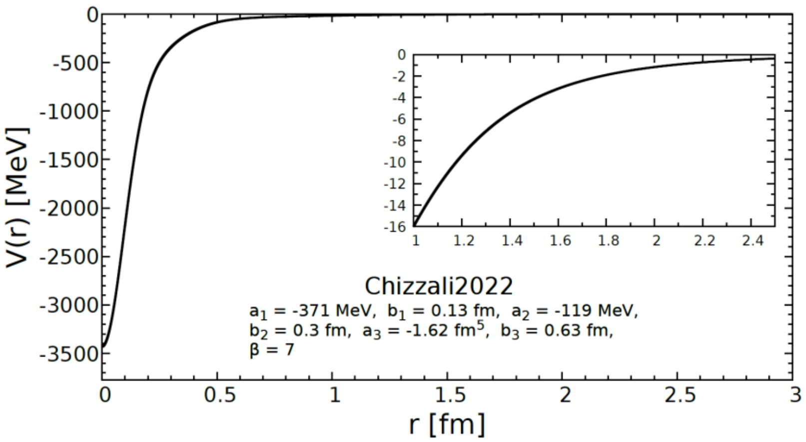

$a_0 = 1.99$ fm
$r_{\text{eff}} = 0.46$ fm
A bound state

$^2S_{1/2}$ Channel

Parameterised potential E. Chizzali *et al.*, PLB **848**, 138358 (2023)

Channel-couplings are neglected for simplicity

$$V^{(1/2)}(r) = \beta\left[a_1 e^{-(r/b_1)^2} + a_2 e^{-(r/b_2)^2}\right] + a_3 m_\pi^4 f(r; b_3)\frac{e^{-2m_\pi r}}{r^2}$$

Short-range interaction — TPE

Only one adjustable parameter β

default: $\beta = 7$

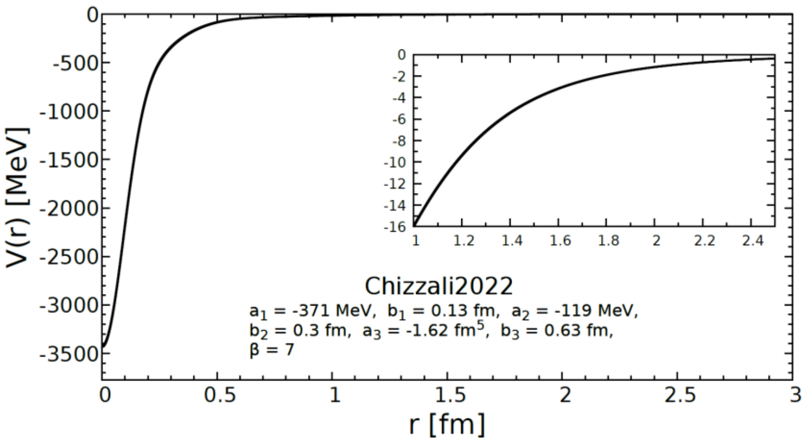

$a_0 = 1.99$ fm

$r_{\text{eff}} = 0.46$ fm

A bound state

WF: $|\varphi_0|^2 - (j_0)^2$

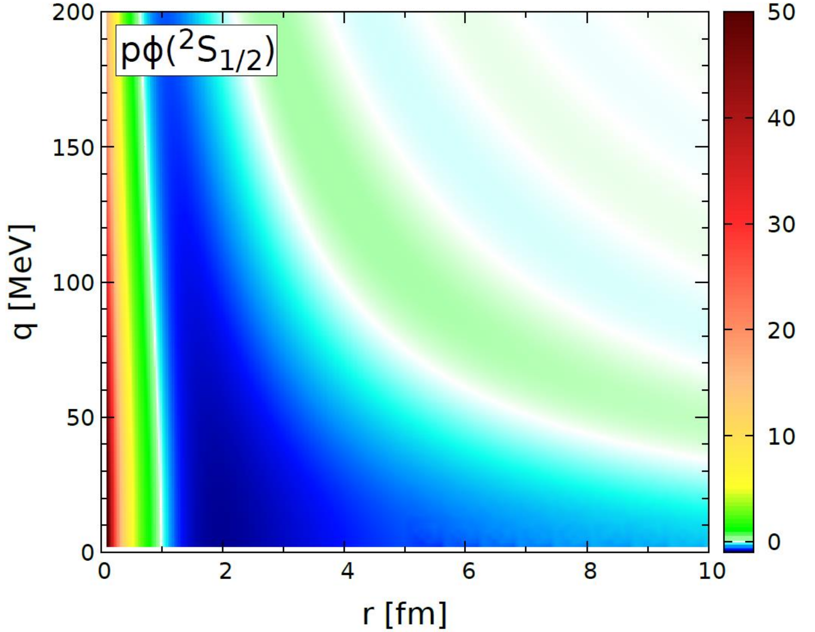

- **Strong enhancement at small qr**
- **"Negative valley" around a_0**

Dynamical Core–Corona Initialisation model (DCCI2)

Y. Kanakubo, Y. Tachibana, and T. Hirano, PRC **105**, 024905 (2022)

A state-of-the-art dynamical model based on core–corona picture

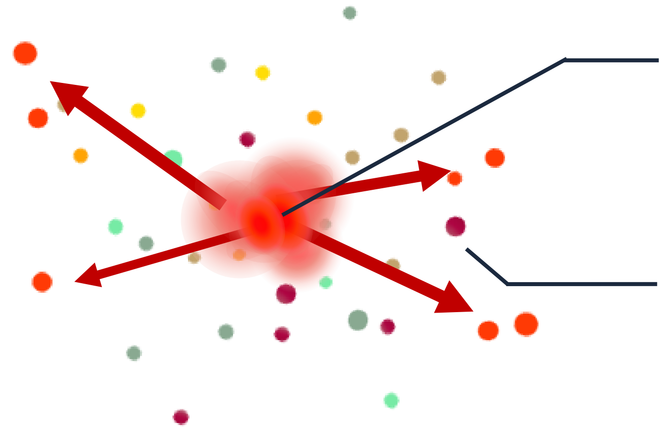

Core:
Equilibrated matter ~ QGP

Corona:
Non-equilibrium partons

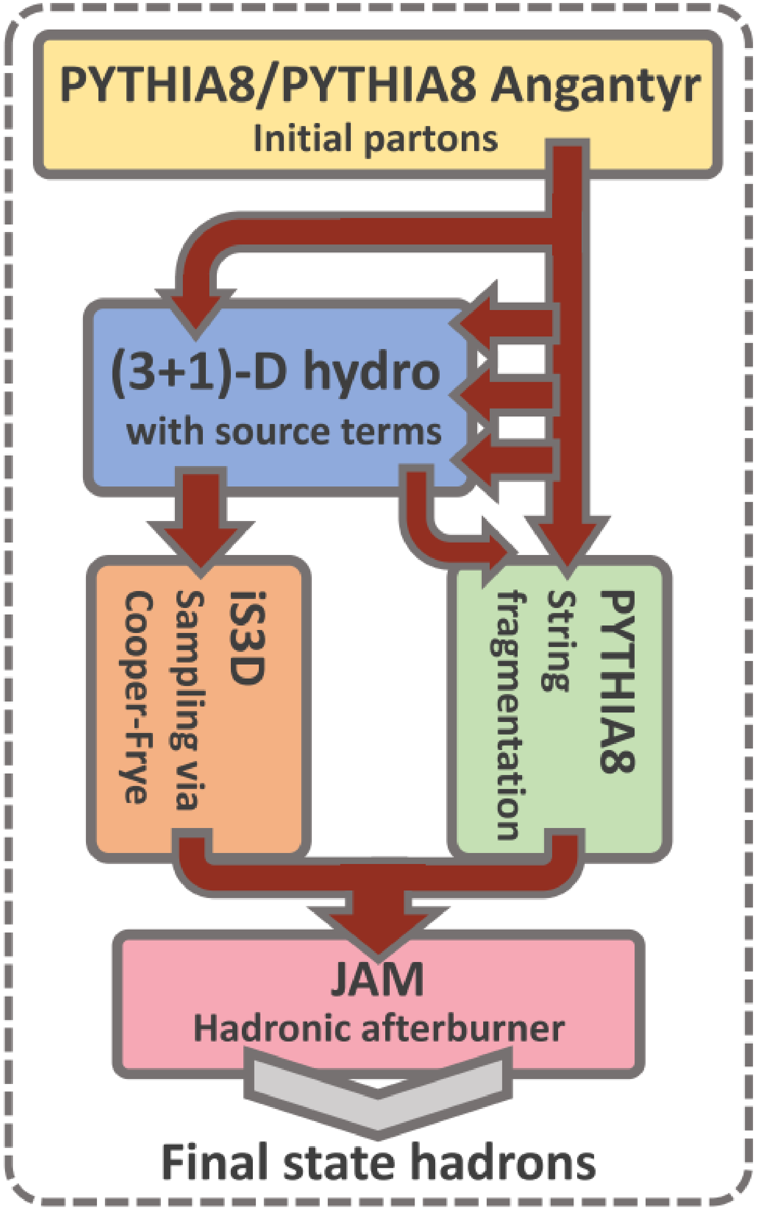

Dynamical Core–Corona Initialisation model (DCCI2)

Y. Kanakubo, Y. Tachibana, and T. Hirano, PRC **105**, 024905 (2022)

A state-of-the-art dynamical model based on core–corona picture

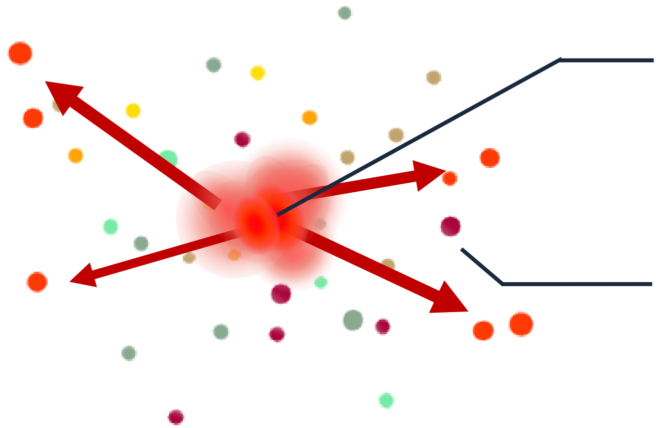

Core:
Equilibrated matter ~ QGP

Corona:
Non-equilibrium partons

Applicable to HM p+p collisions

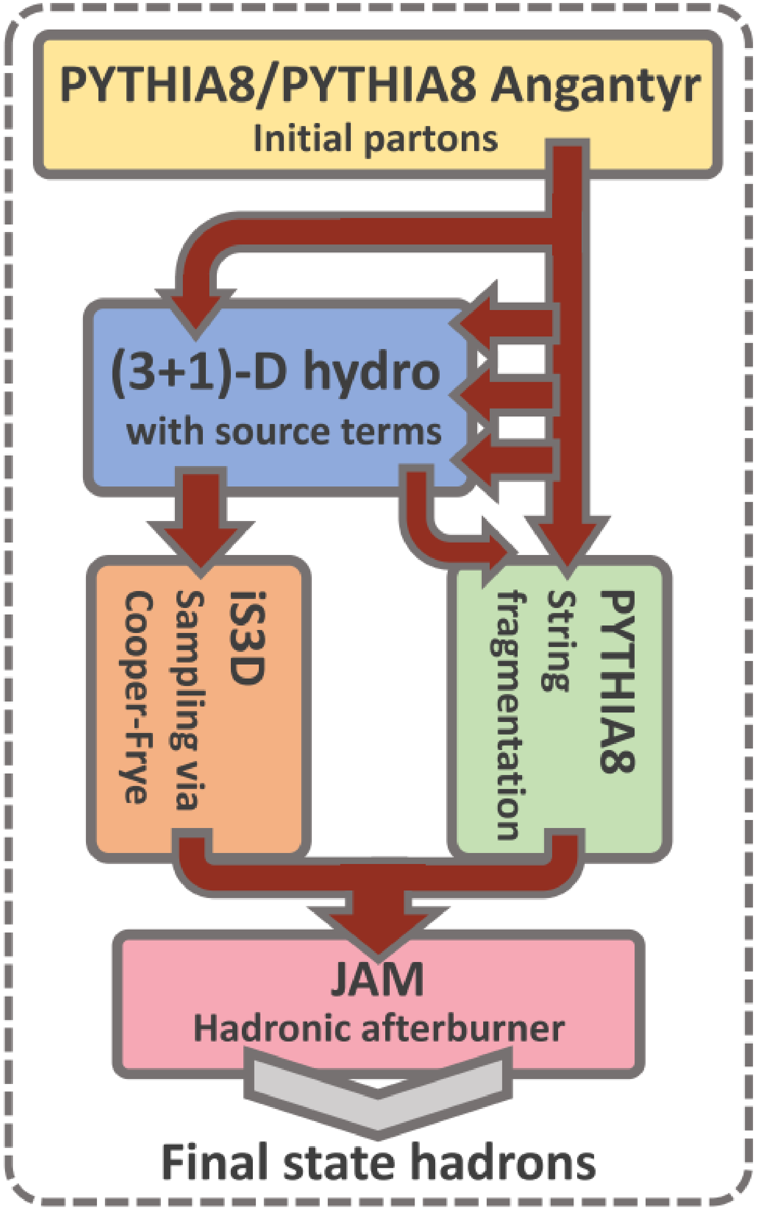

How DCCI2 works

HM p+p collisions at $\sqrt{s} = 7$ TeV

Movies: Courtesy of Y. Kanakubo

Transverse plane

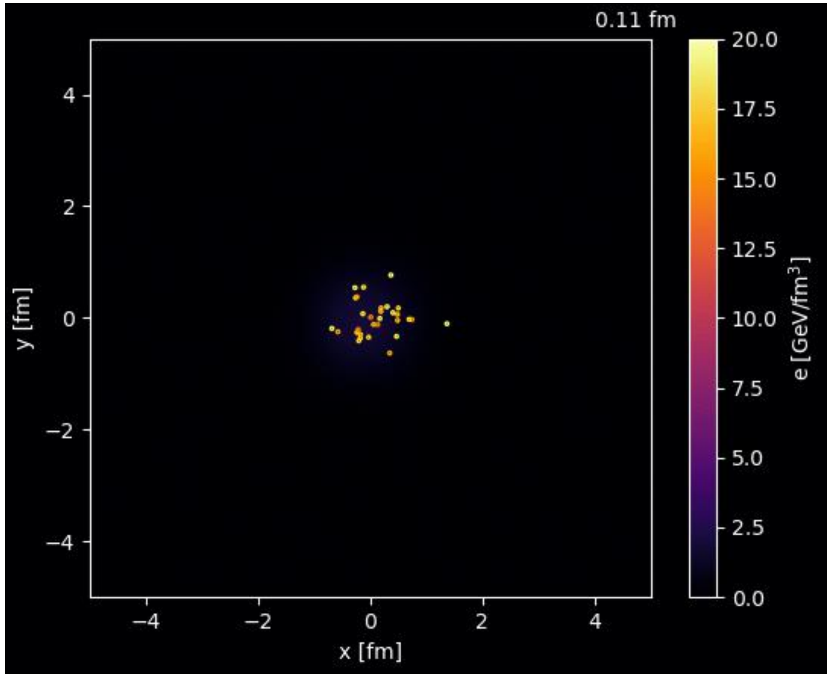

x–η_s plane

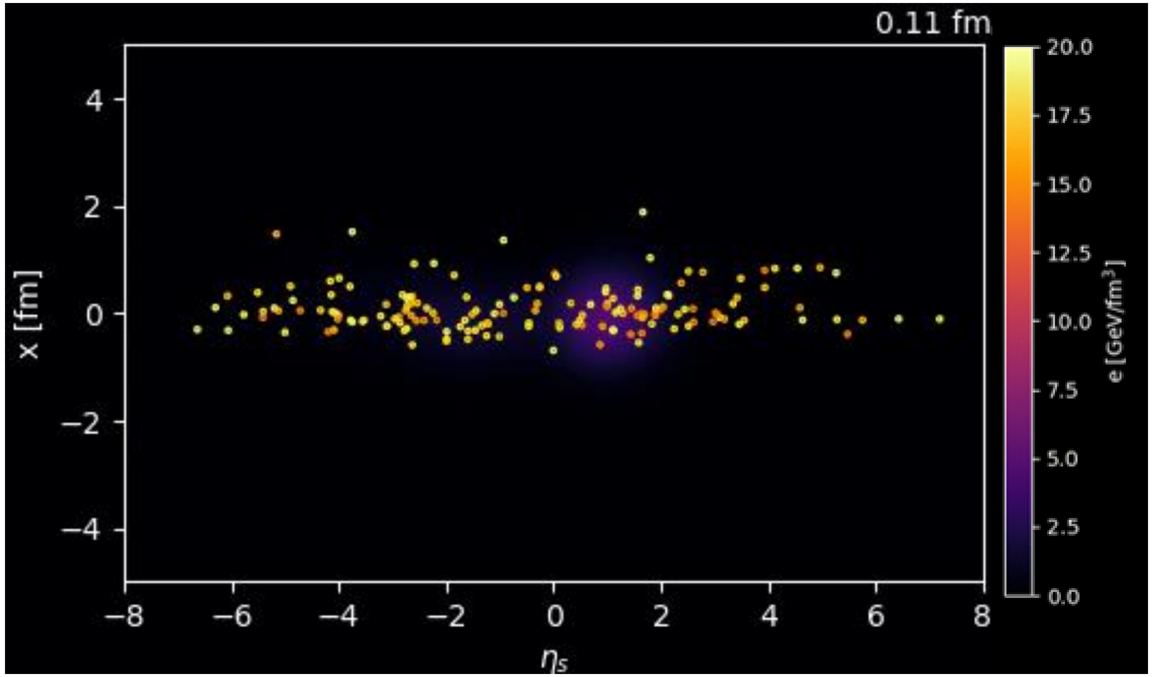

Describe the space-time evolution of nuclear collisions

→ SF that reflects collision dynamics

How DCCI2 works

HM p+p collisions at $\sqrt{s} = 7$ TeV

Movies: Courtesy of Y. Kanakubo

Transverse plane

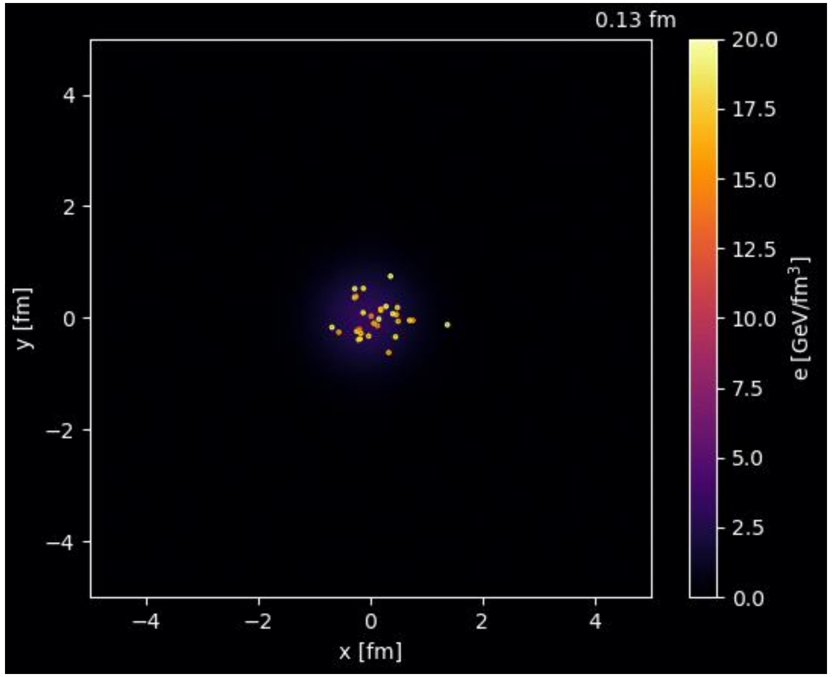

x–η_s plane

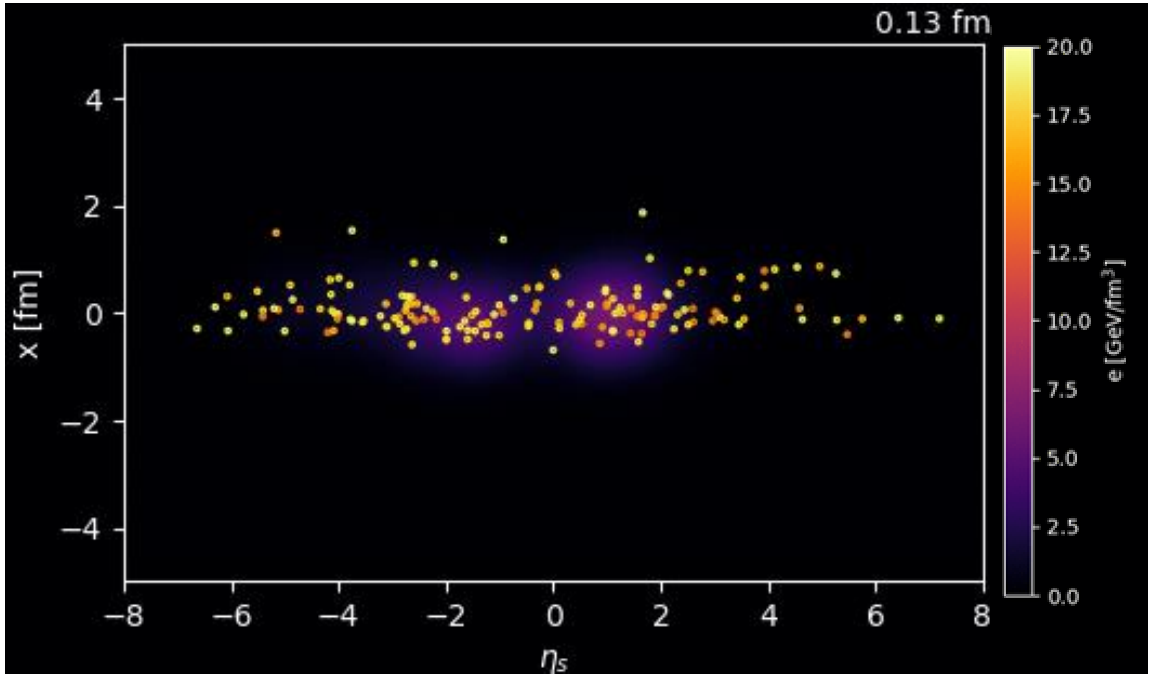

Describe the space-time evolution of nuclear collisions

→ SF that reflects collision dynamics

How DCCI2 works

HM p+p collisions at $\sqrt{s} = 7$ TeV

Movies: Courtesy of Y. Kanakubo

Transverse plane

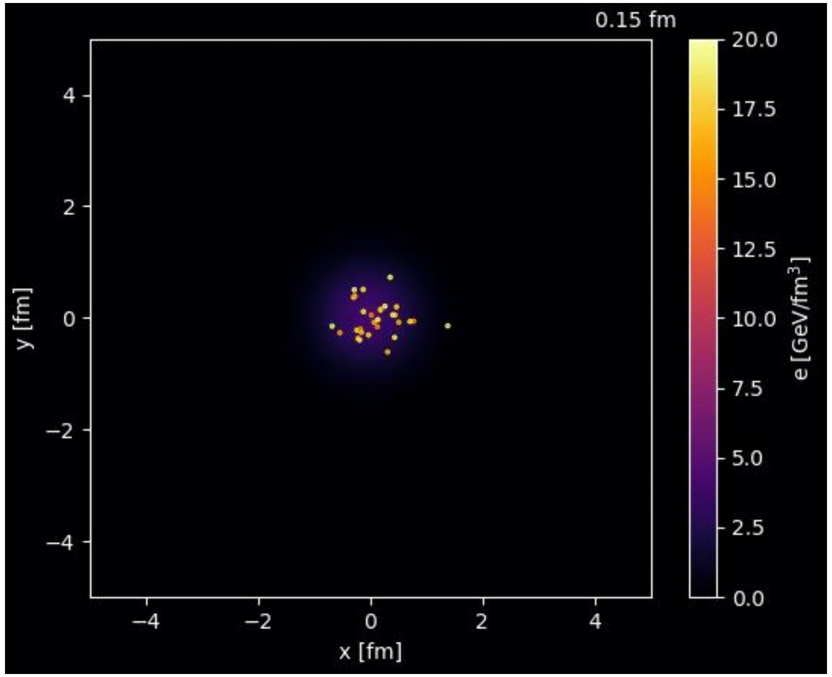

x–η_s plane

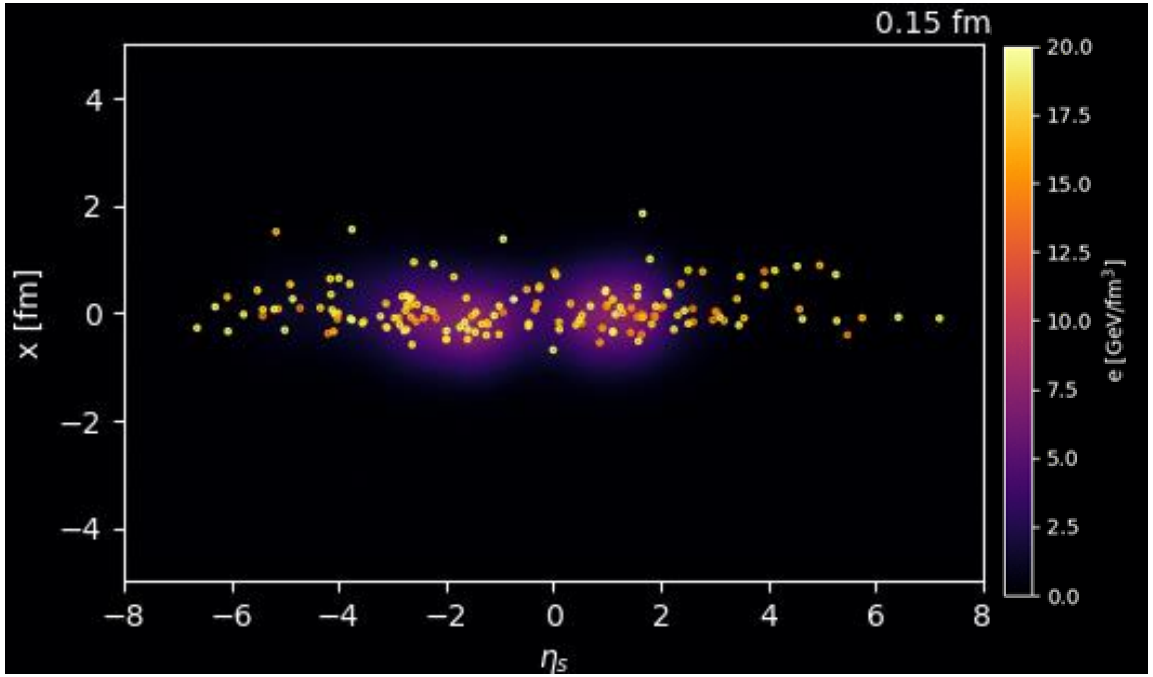

Describe the space-time evolution of nuclear collisions

→ SF that reflects collision dynamics

How DCCI2 works

HM p+p collisions at $\sqrt{s} = 7$ TeV

Movies: Courtesy of Y. Kanakubo

Transverse plane

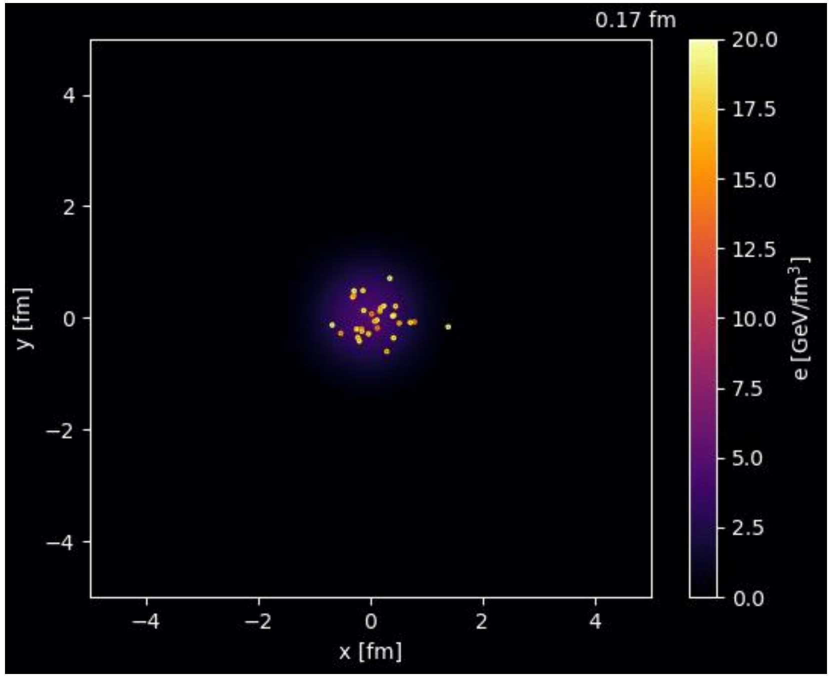

x–η_s plane

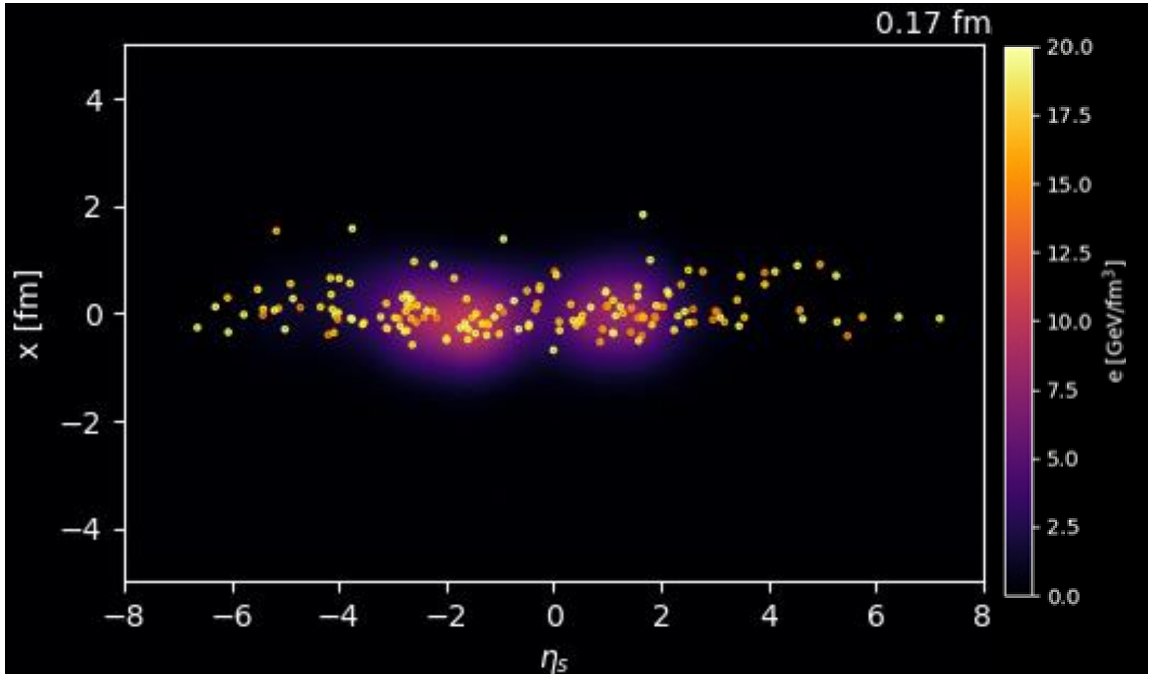

Describe the space-time evolution of nuclear collisions

→ SF that reflects collision dynamics

How DCCI2 works

HM p+p collisions at $\sqrt{s} = 7$ TeV

Movies: Courtesy of Y. Kanakubo

Transverse plane

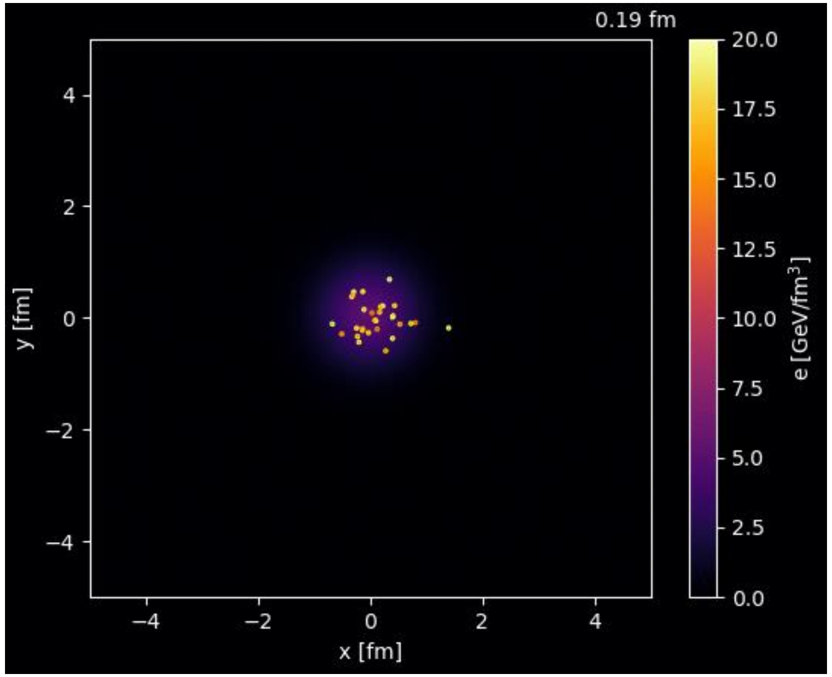

x–η_s plane

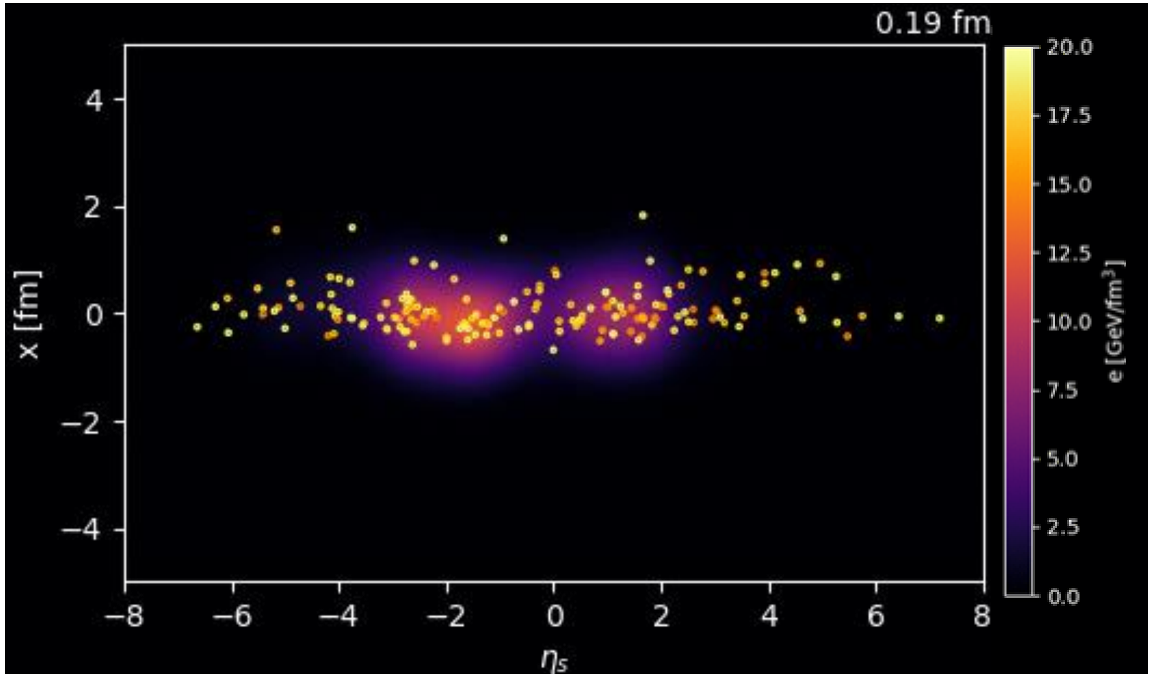

Describe the space-time evolution of nuclear collisions

→ SF that reflects collision dynamics

How DCCI2 works

HM p+p collisions at $\sqrt{s} = 7$ TeV

Movies: Courtesy of Y. Kanakubo

Transverse plane

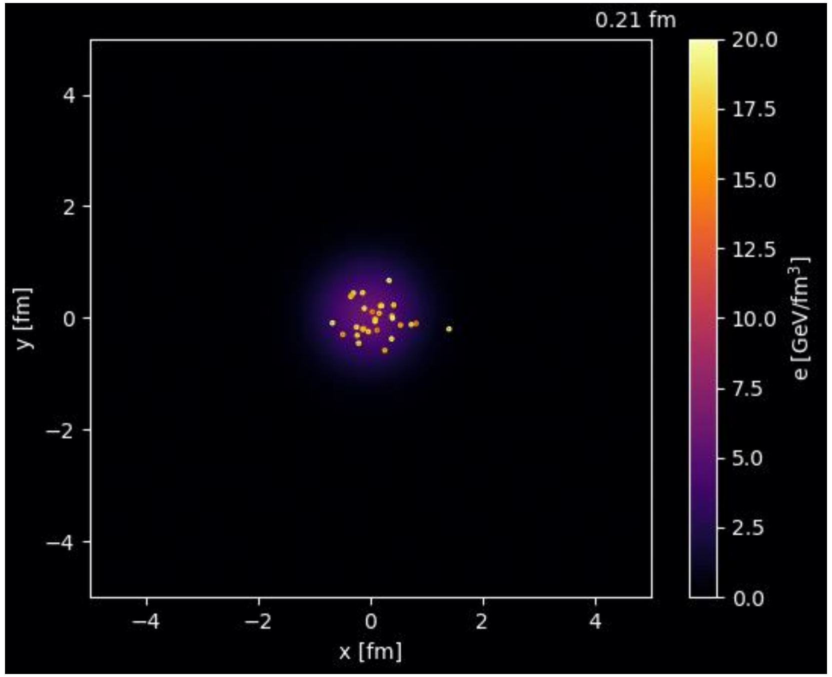

x–η_s plane

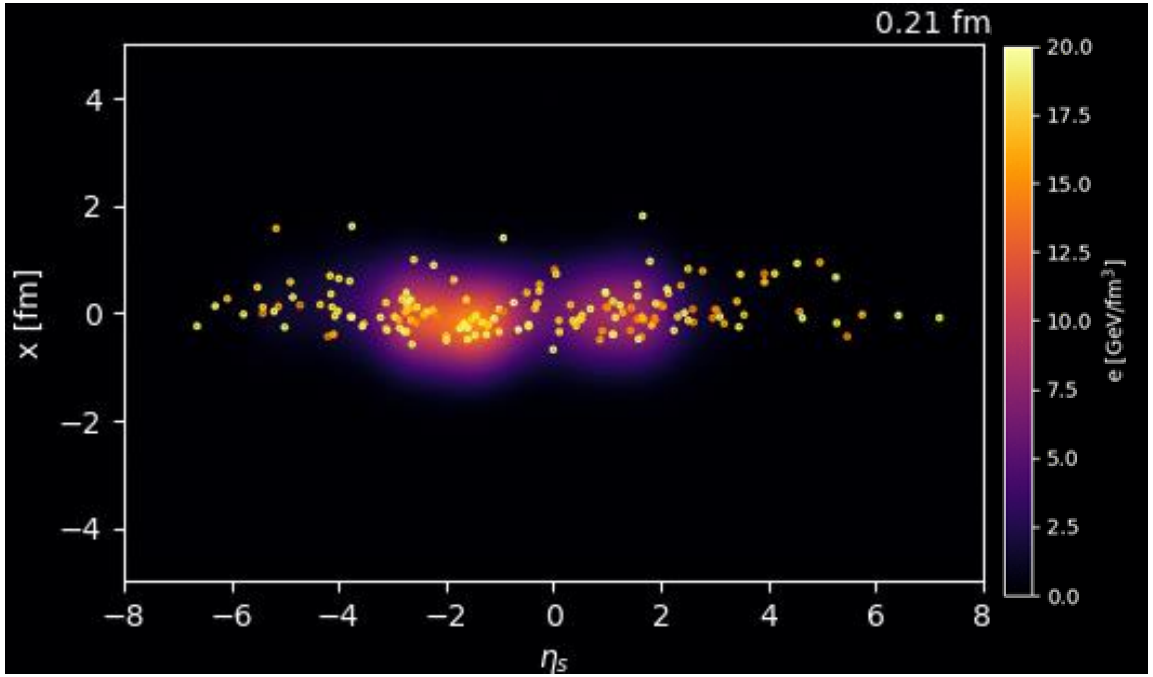

Describe the space-time evolution of nuclear collisions

→ SF that reflects collision dynamics

How DCCI2 works

HM p+p collisions at $\sqrt{s} = 7$ TeV

Movies: Courtesy of Y. Kanakubo

Transverse plane

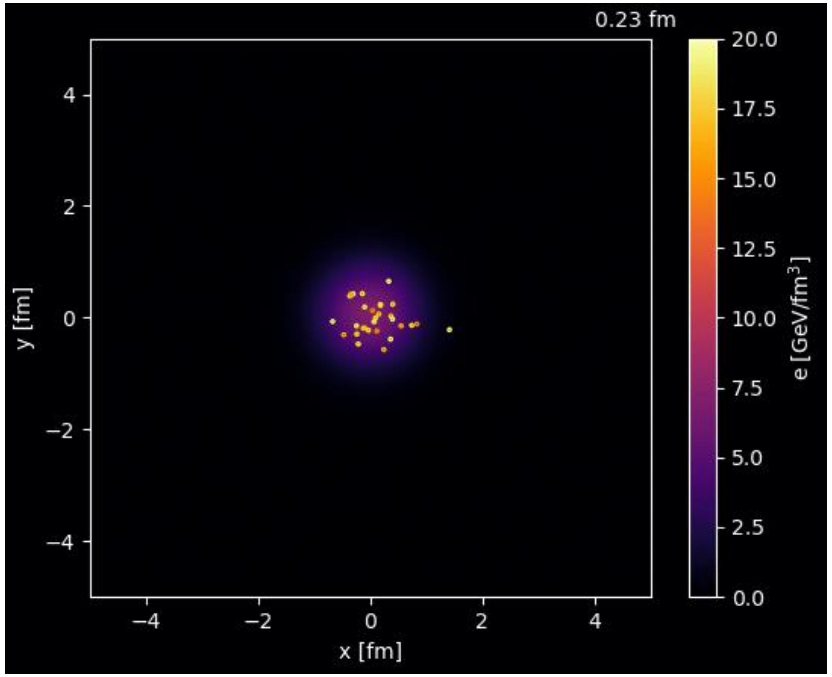

x–η_s plane

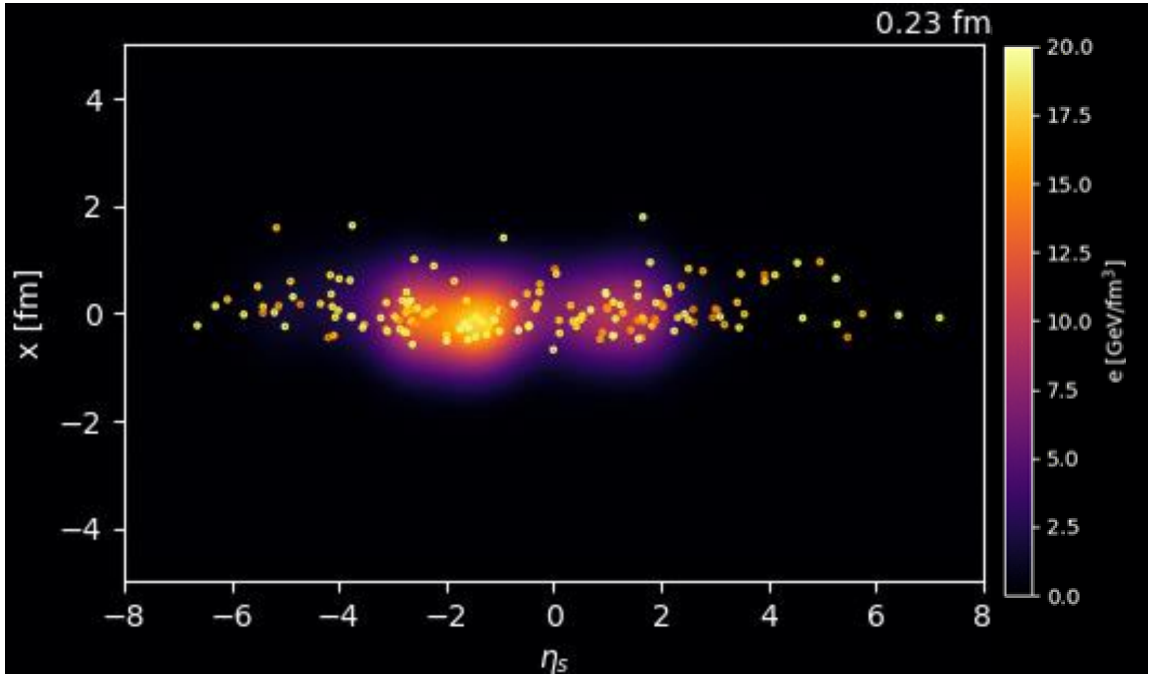

Describe the space-time evolution of nuclear collisions

→ SF that reflects collision dynamics

How DCCI2 works

HM p+p collisions at $\sqrt{s} = 7$ TeV

Movies: Courtesy of Y. Kanakubo

Transverse plane

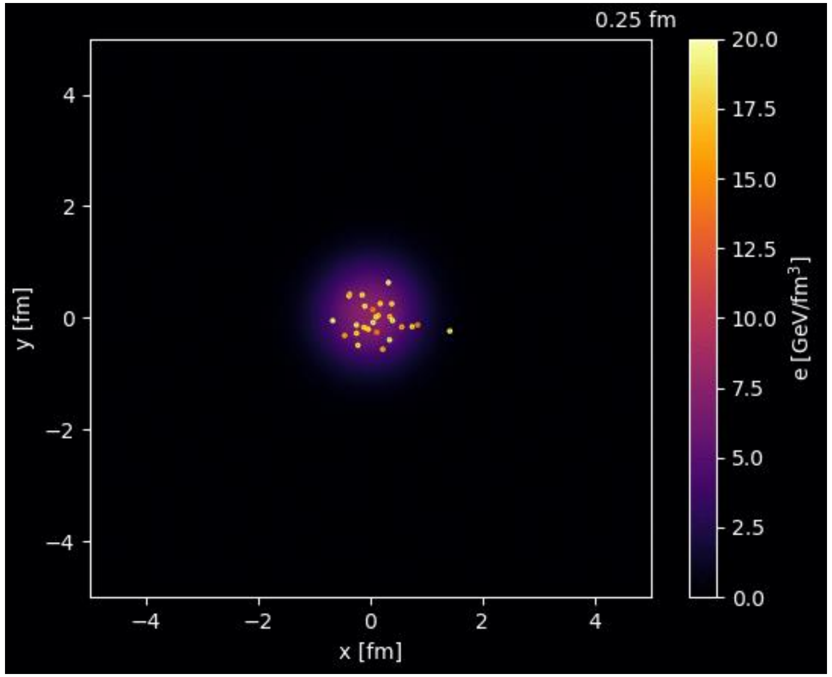

x–η_s plane

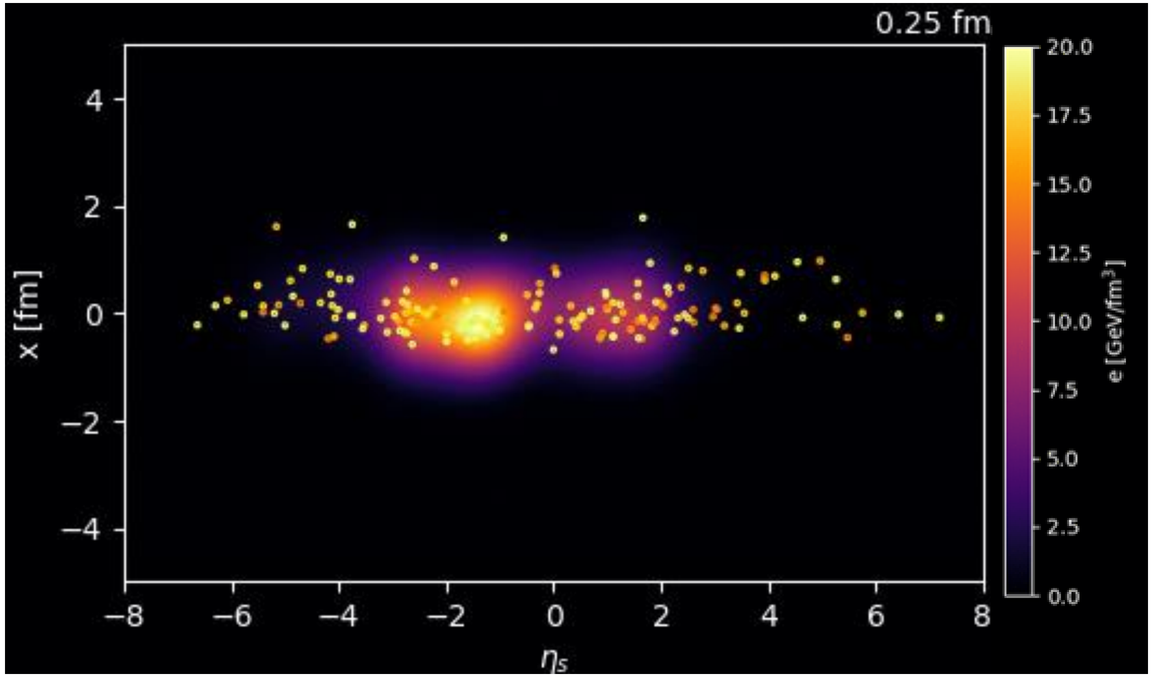

Describe the space-time evolution of nuclear collisions

→ SF that reflects collision dynamics

How DCCI2 works

HM p+p collisions at $\sqrt{s} = 7$ TeV

Movies: Courtesy of Y. Kanakubo

Transverse plane

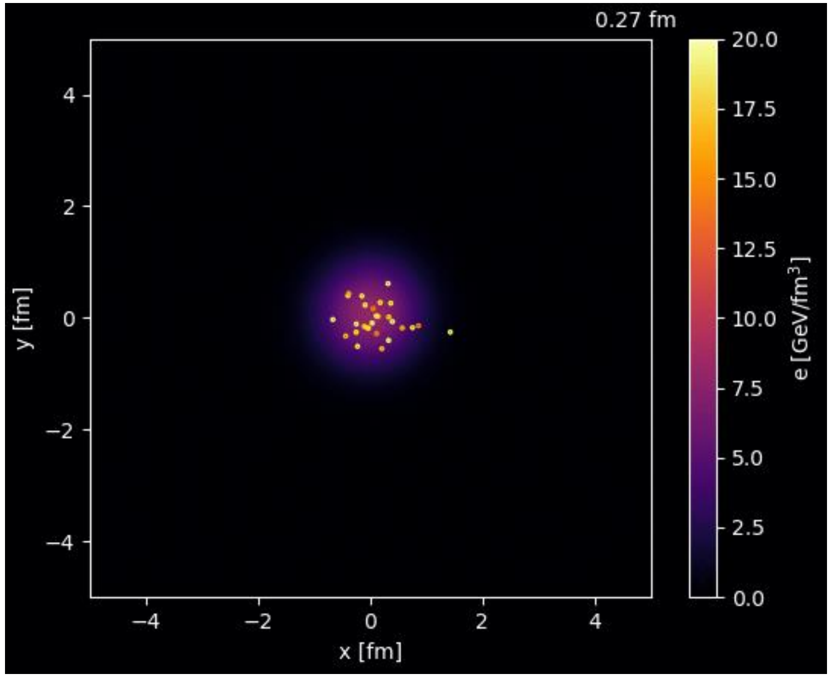

x–η_s plane

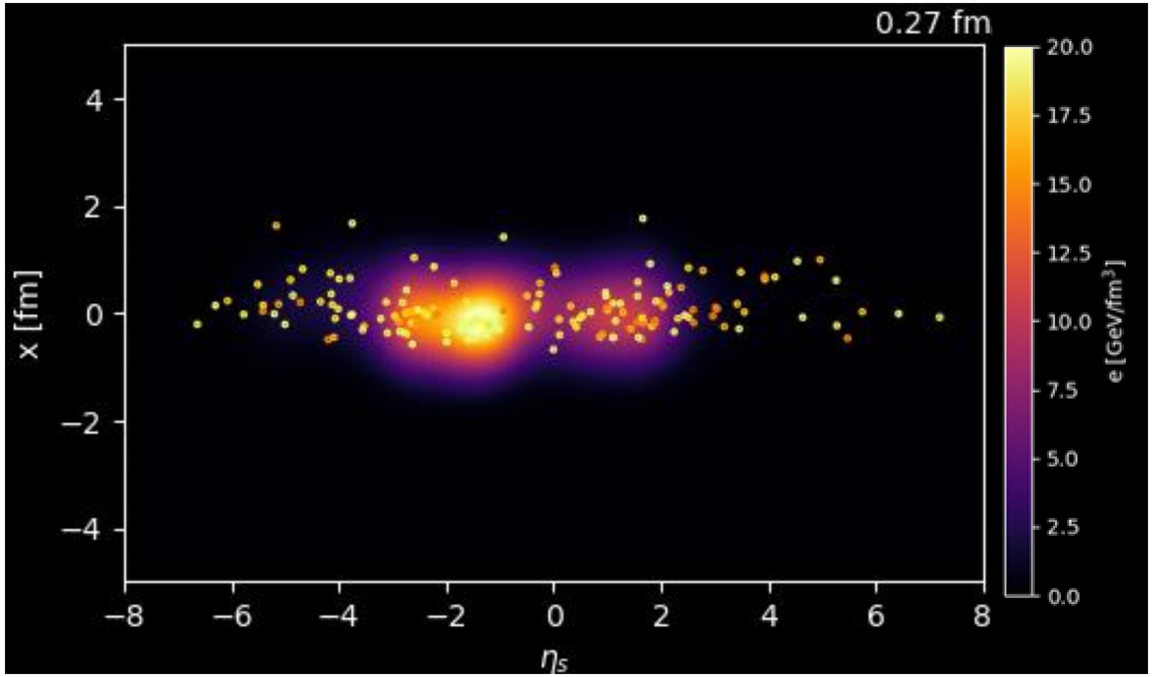

Describe the space-time evolution of nuclear collisions

→ SF that reflects collision dynamics

How DCCI2 works

HM p+p collisions at $\sqrt{s} = 7$ TeV

Movies: Courtesy of Y. Kanakubo

Transverse plane

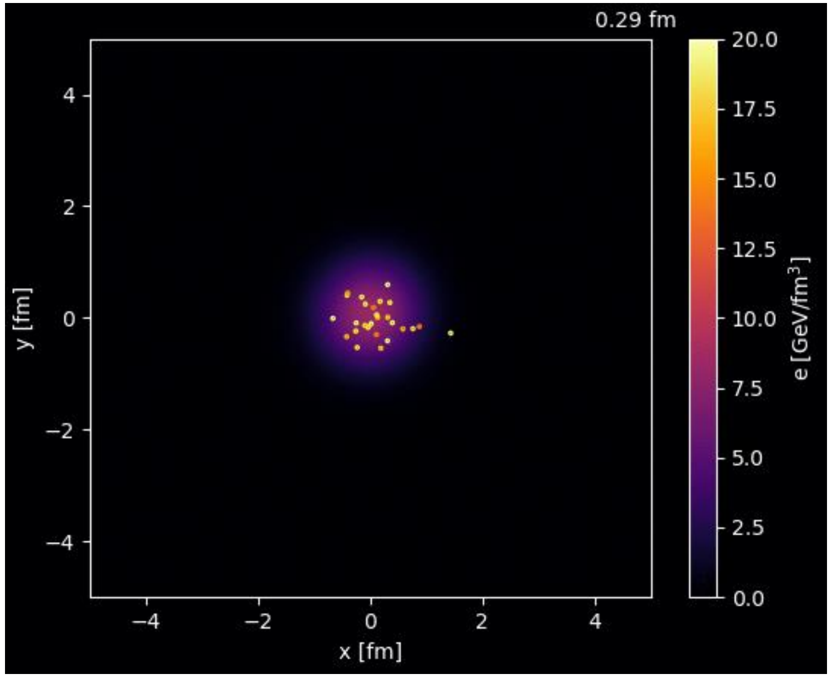

x–η_s plane

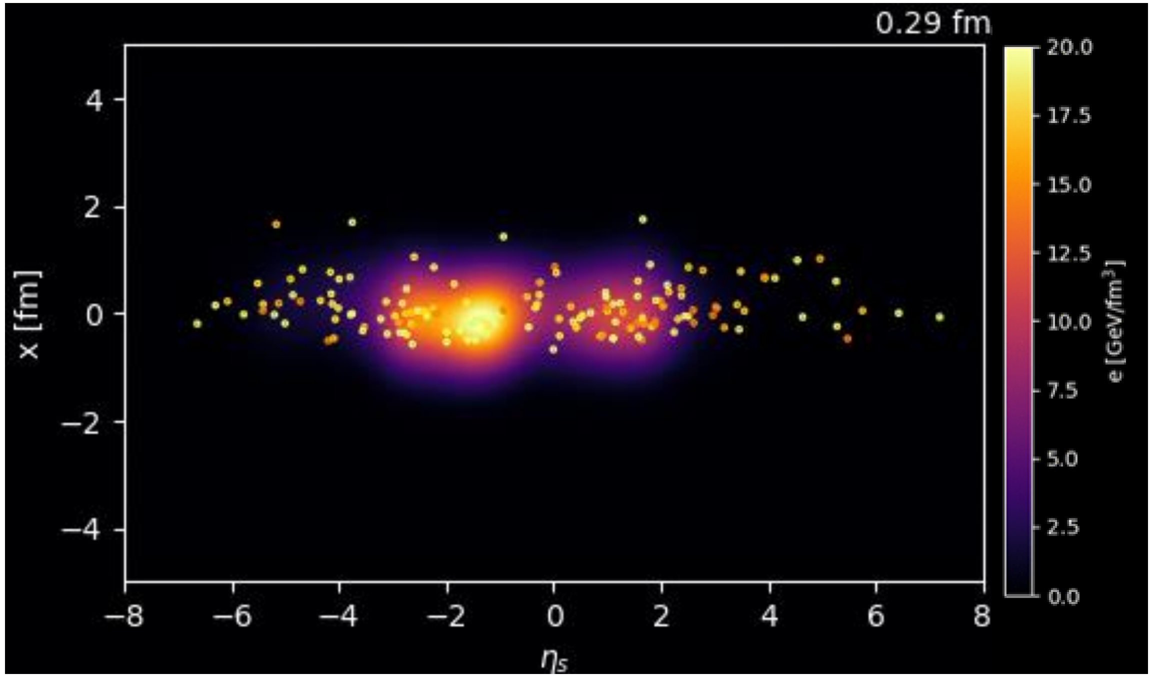

Describe the space-time evolution of nuclear collisions

→ SF that reflects collision dynamics

Source function from DCCI2

q-integrated SF

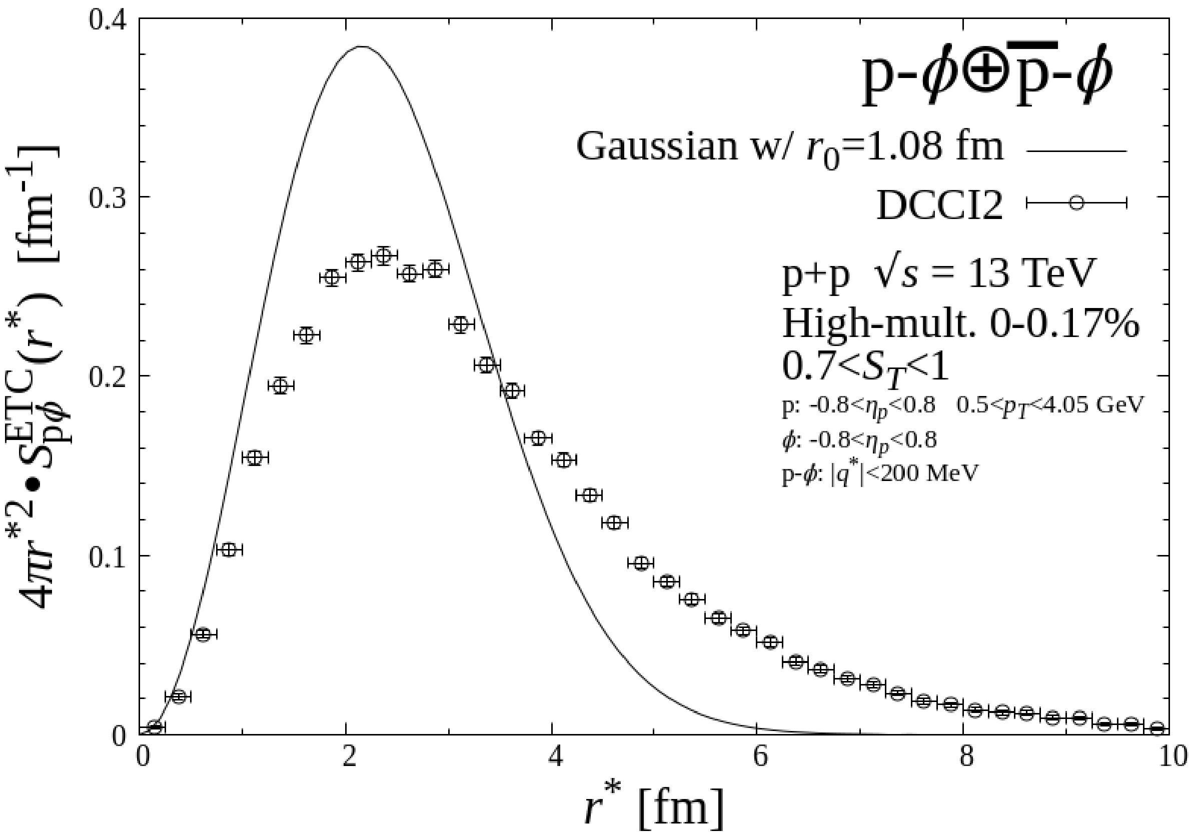

Source function from DCCI2

q-integrated SF

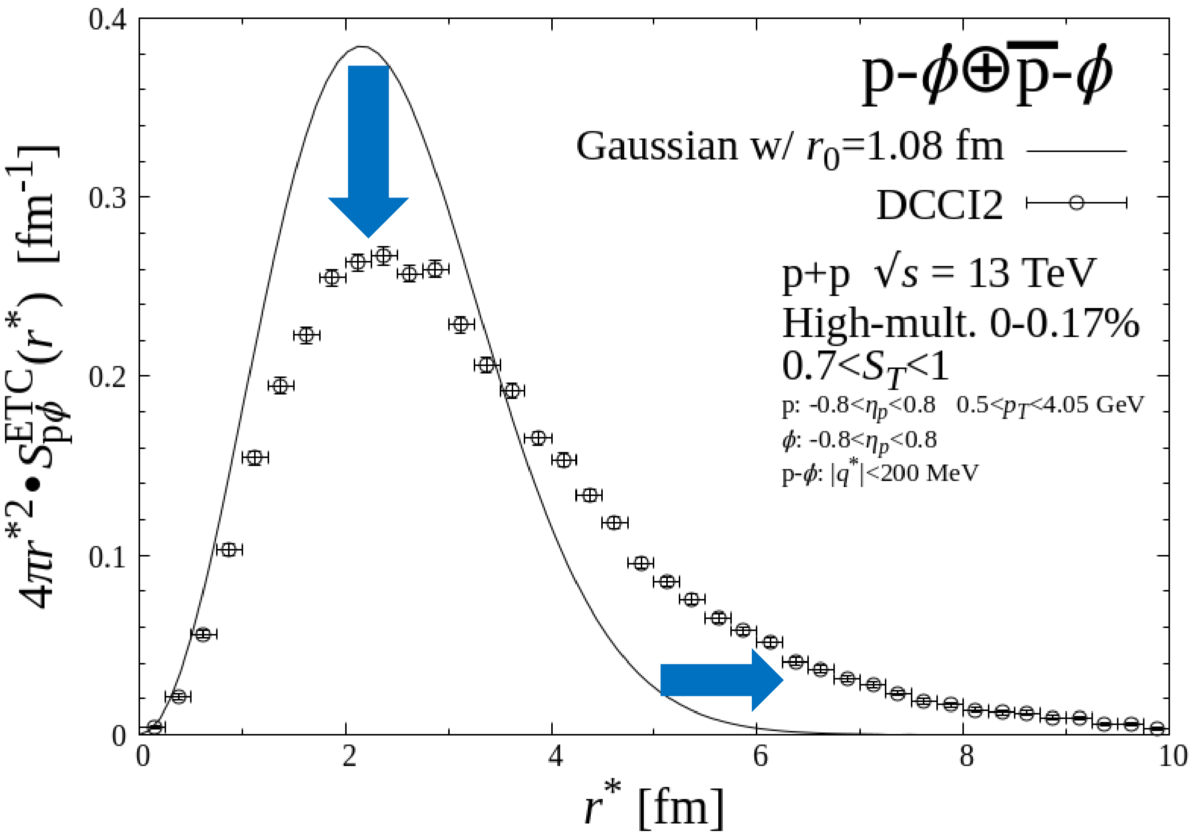

Larger source size $\langle r^2 \rangle$

mainly from hadronic rescatterings

Source function from DCCI2

q-integrated SF

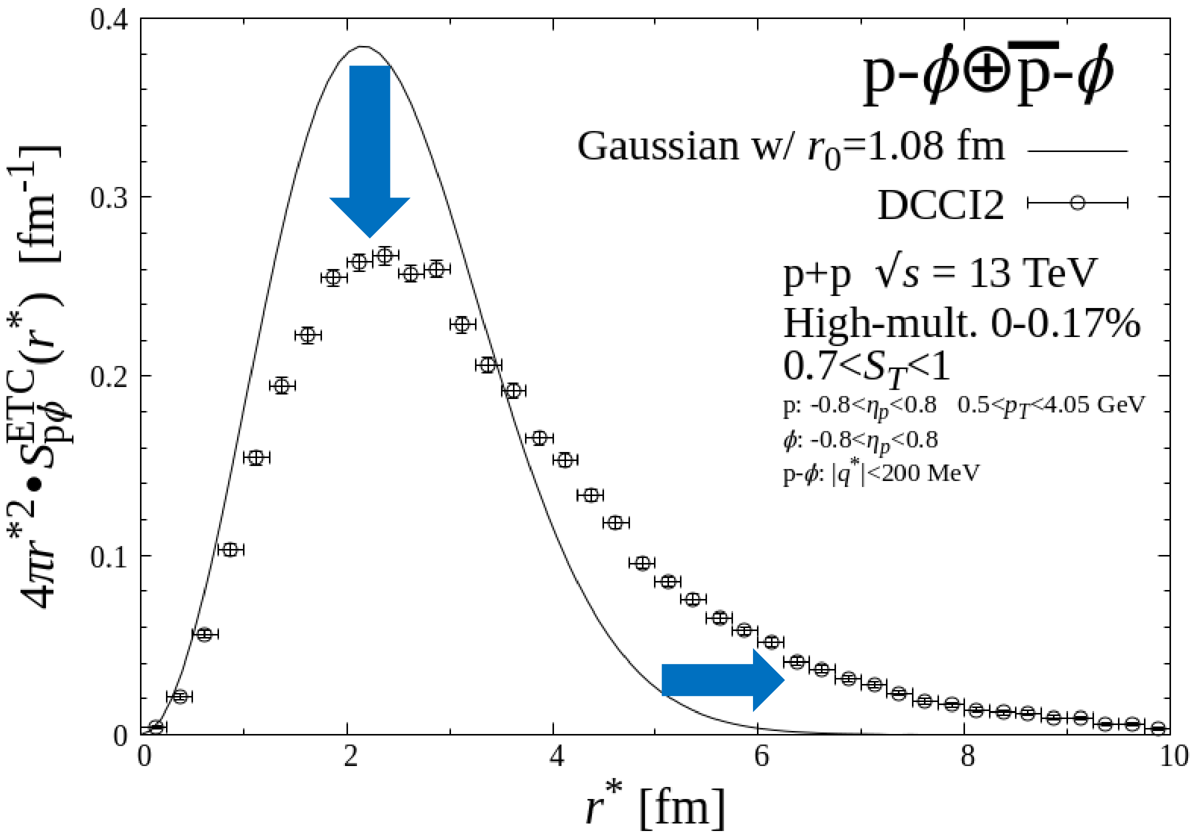

Larger source size $\langle r^2 \rangle$

mainly from hadronic rescatterings

q-differential SF

SF generally depends on q due to e.g., collectivity

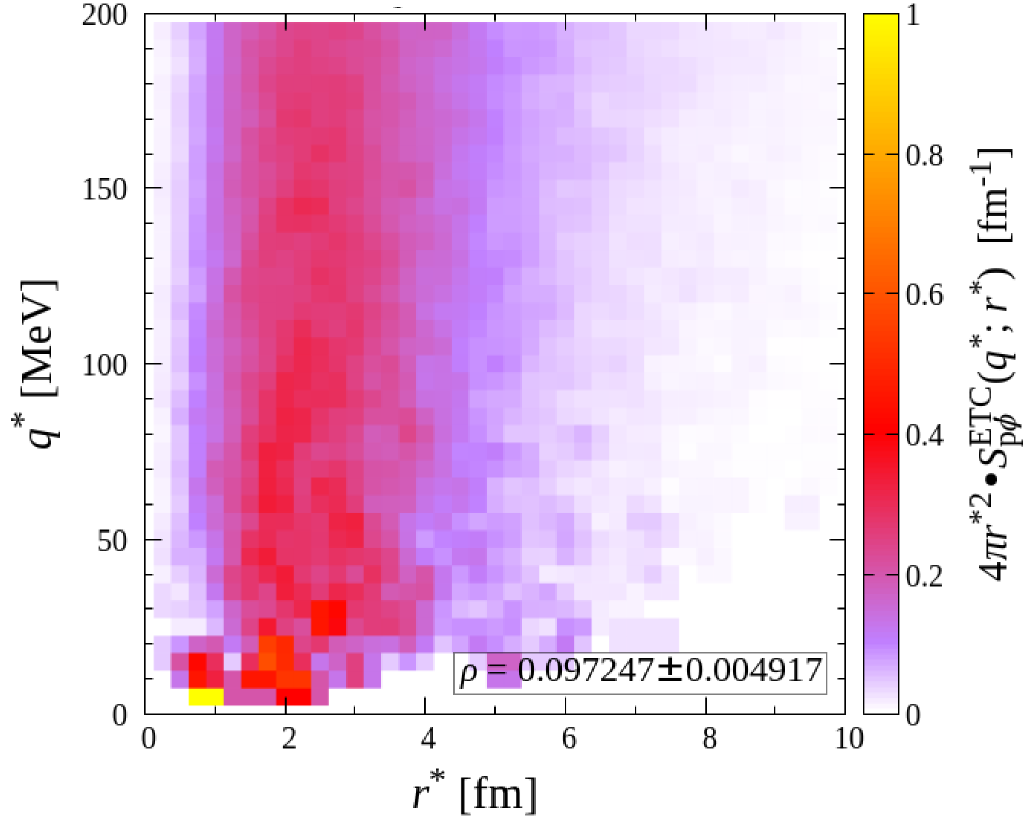

Source function from DCCI2

q-integrated SF

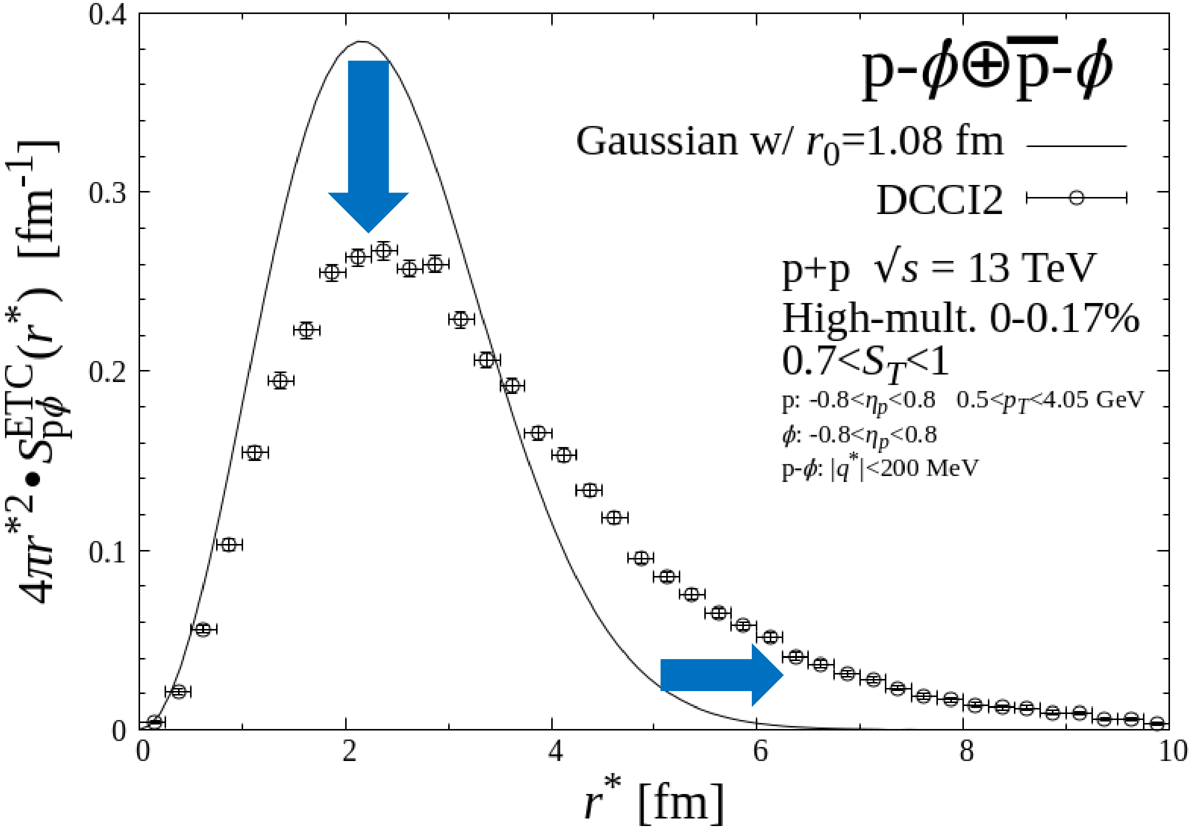

Larger source size $\langle r^2 \rangle$

mainly from hadronic rescatterings

q-differential SF

SF generally depends on *q* due to e.g., collectivity

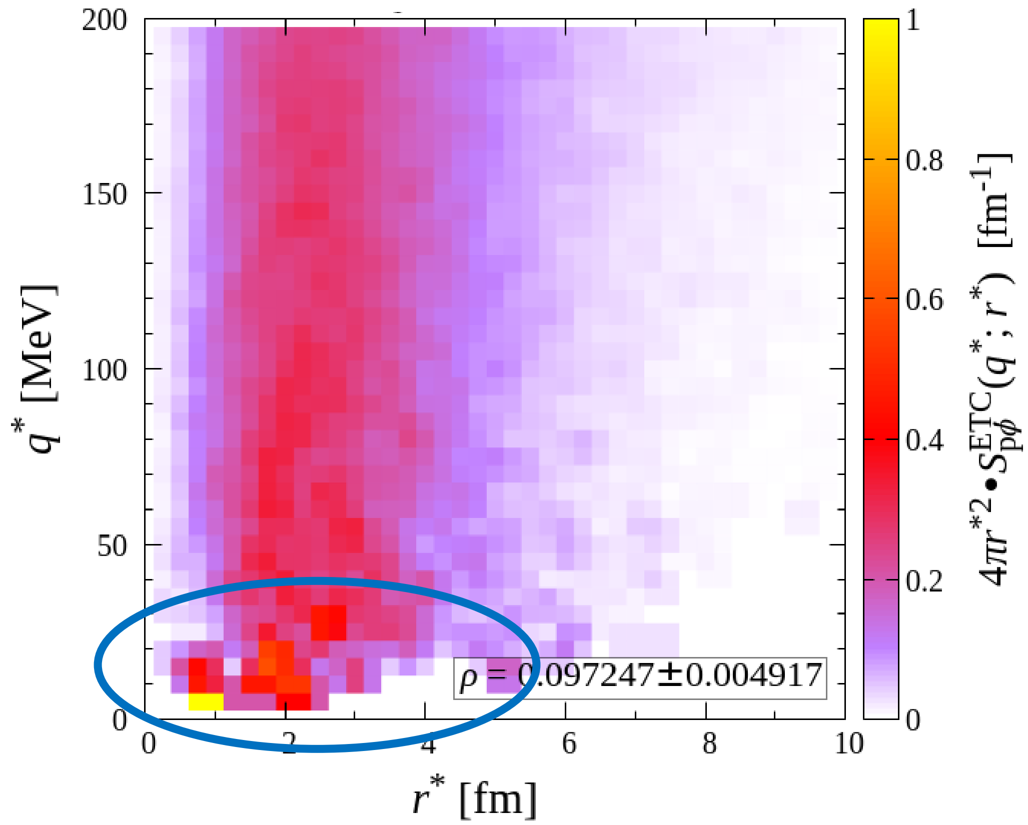

Noticeably smaller source

Correlation function from DCCI2

Green: $C^{(3/2)}$, Blue: $C^{(1/2)}$, Red: $C^{\mathrm{tot}} = \frac{2}{3}C^{(3/2)} + \frac{1}{3}C^{(1/2)}$

Plots: **DCCI2 SF**, Lines: Gaussian SF ($r_0 = 1.08$ fm)

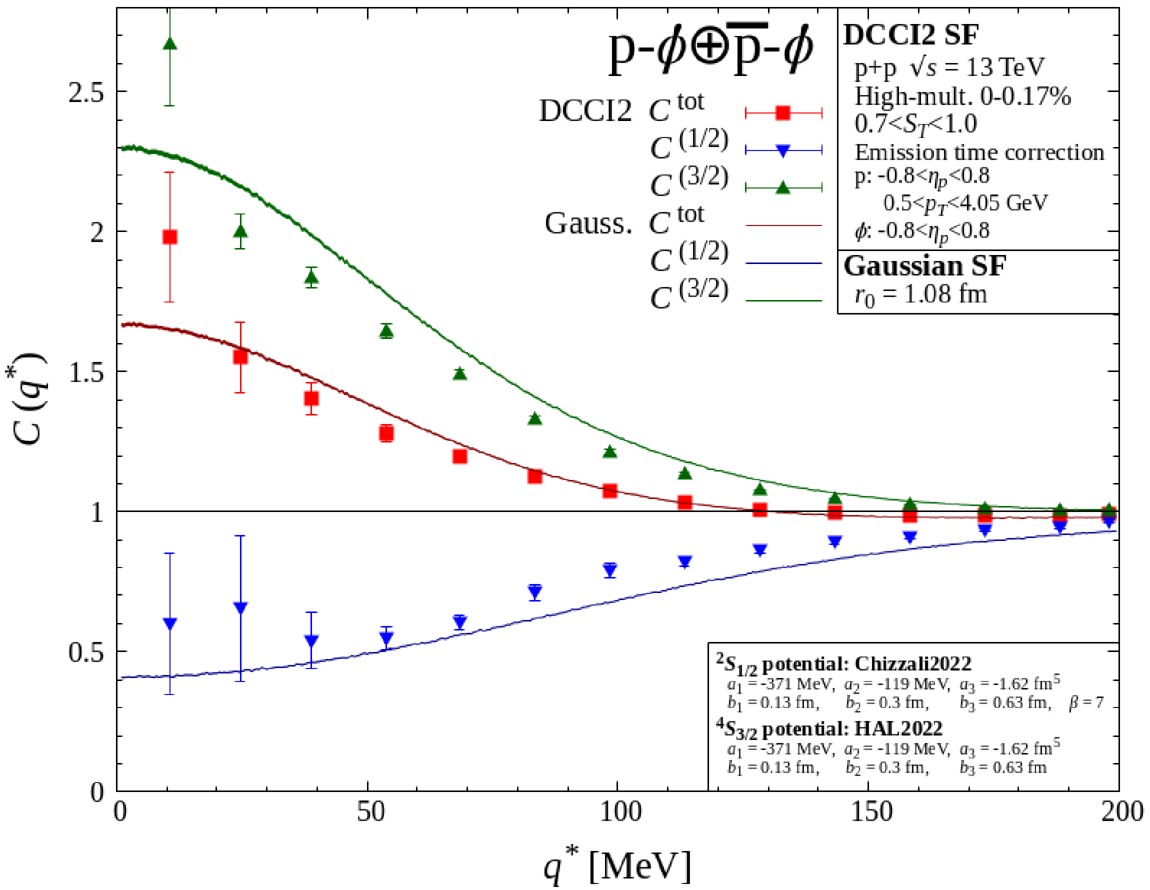

DCCI2 vs. Gaussian

- **Slightly weaker correlation**
- **Non-trivial behaviour at small *q***

Small but statistically significant effects of collision dynamics

Compare with ALICE data

$C^{(3/2)}$: Fixed, $C^{(1/2)}$: Change with β

Compare $C^{\mathrm{tot}} = \frac{2}{3}C^{(3/2)} + \frac{1}{3}C^{(1/2)}$ with ALICE data

Compare with ALICE data

$C^{(3/2)}$: Fixed, $C^{(1/2)}$: Change with β

Compare $C^{\mathrm{tot}} = \frac{2}{3} C^{(3/2)} + \frac{1}{3} C^{(1/2)}$ with ALICE data

$\beta = 6$

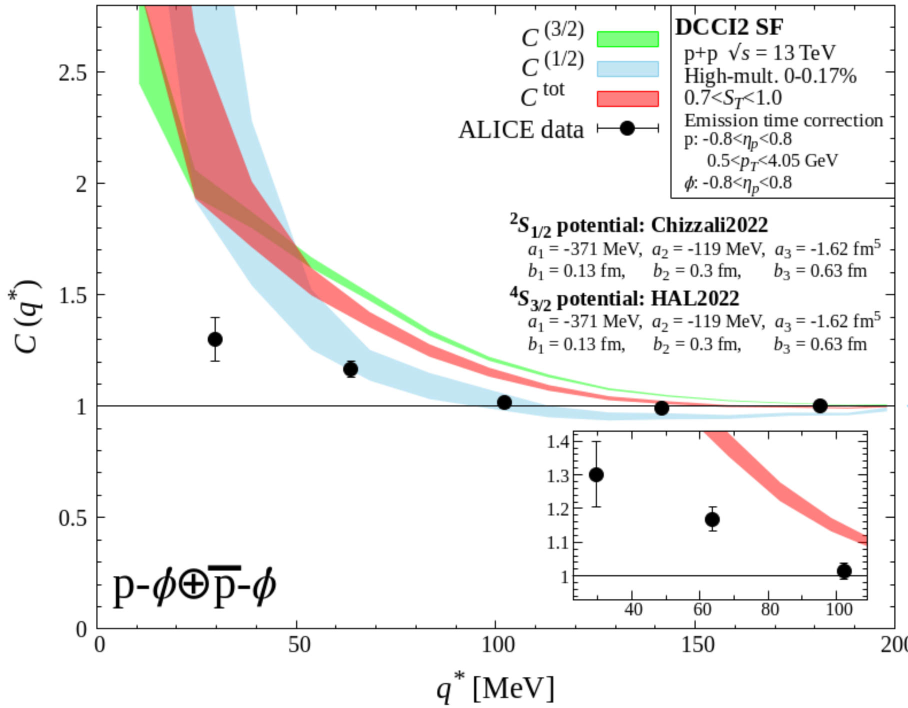

$C^{\mathrm{tot}} > C^{\mathrm{exp}}$

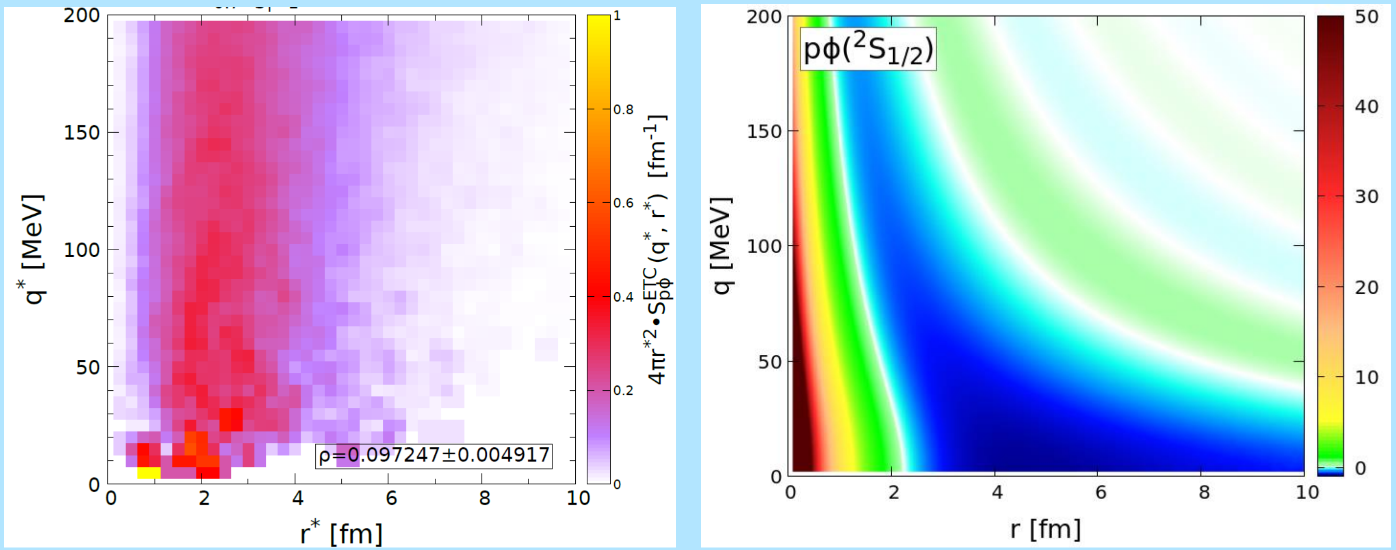

SF picks up strong positive region of WF

Compare with ALICE data

$C^{(3/2)}$: Fixed, $C^{(1/2)}$: Change with β

Compare $C^{\mathrm{tot}} = \frac{2}{3} C^{(3/2)} + \frac{1}{3} C^{(1/2)}$ with ALICE data

$\boldsymbol{\beta = 7}$

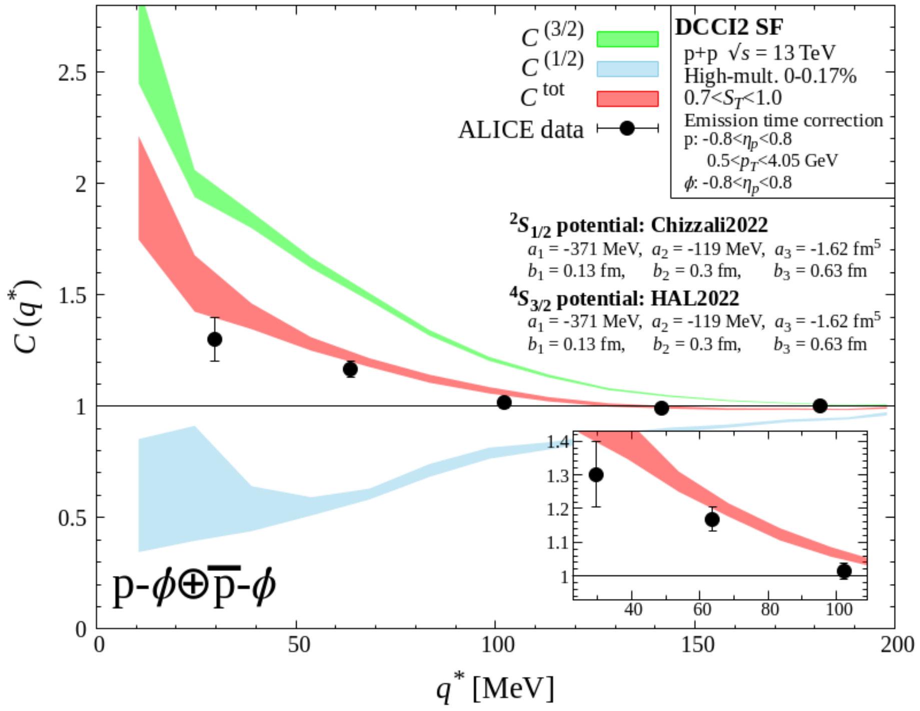

$\boldsymbol{\beta = 8}$

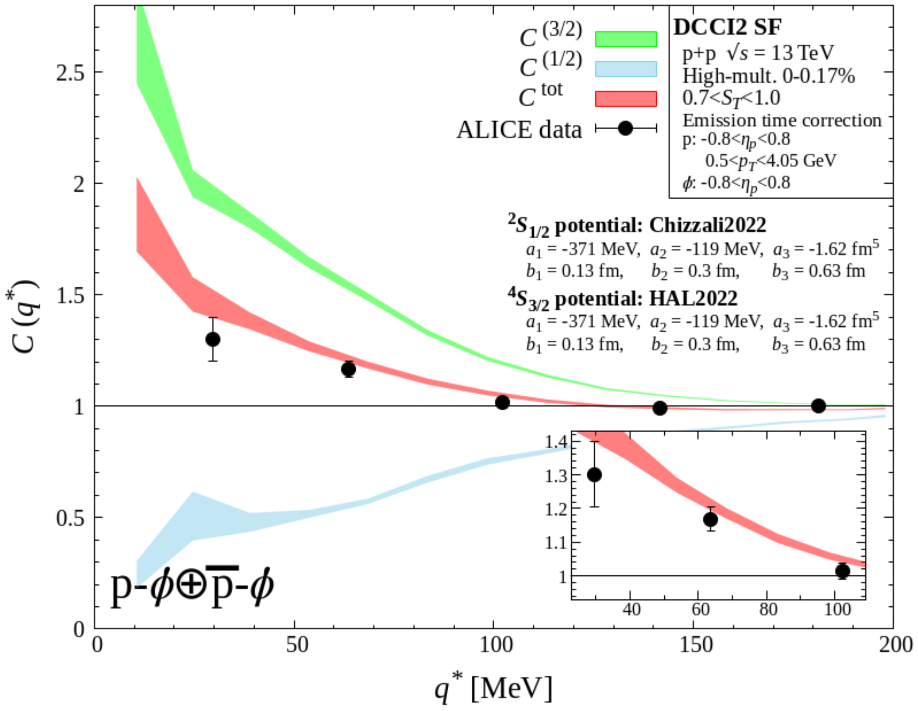

$C^{\mathrm{tot}} \approx C^{\mathrm{exp}}$

Compare with ALICE data

$C^{(3/2)}$: Fixed, $C^{(1/2)}$: Change with β

Compare $C^{\mathrm{tot}} = \frac{2}{3} C^{(3/2)} + \frac{1}{3} C^{(1/2)}$ with ALICE data

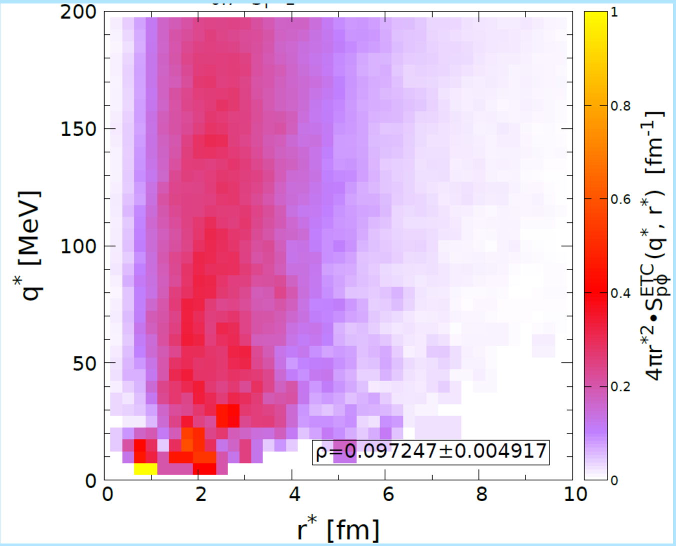

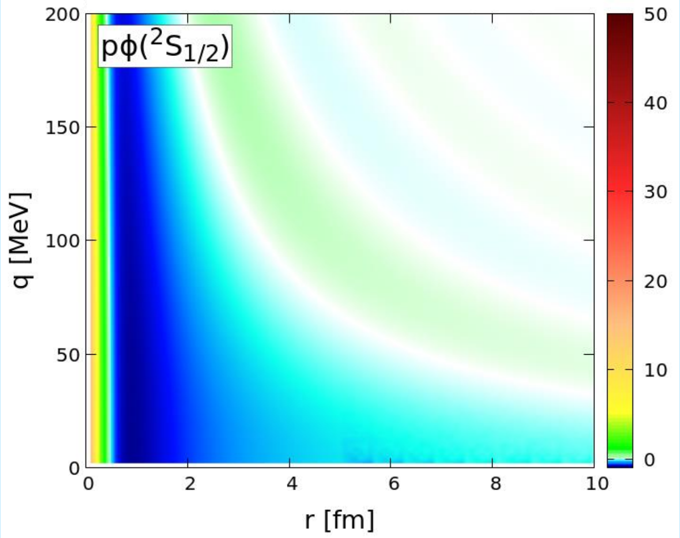

SF cannot pick up negative valley efficiently

$\beta = 9$

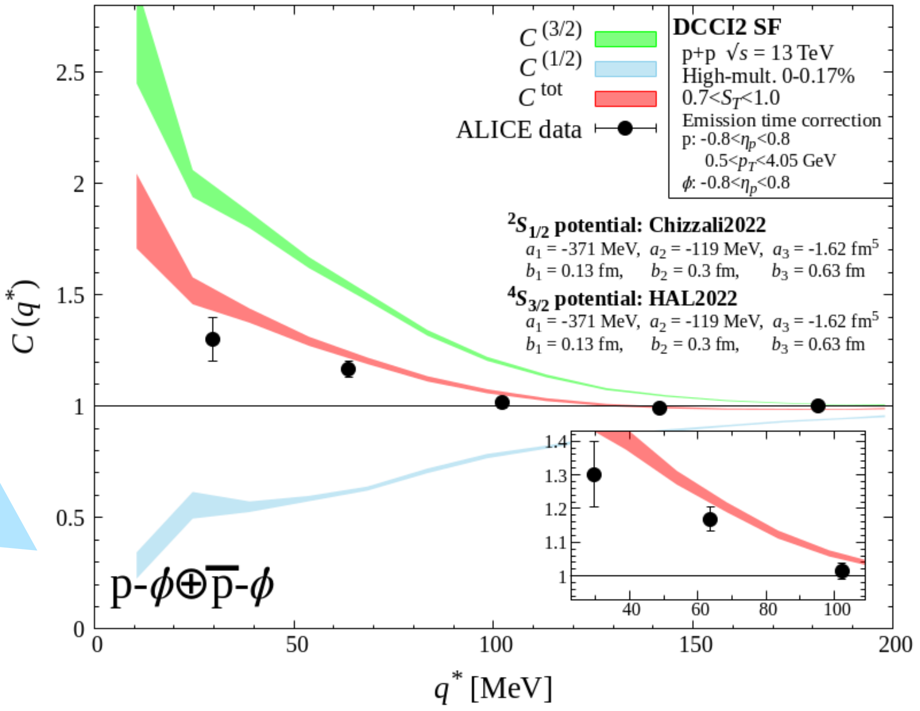

$C^{\mathrm{tot}} > C^{\mathrm{exp}}$

Compare with ALICE data

$C^{(3/2)}$: Fixed, $C^{(1/2)}$: Change with β

Compare $C^{\text{tot}} = \frac{2}{3}C^{(3/2)} + \frac{1}{3}C^{(1/2)}$ with ALICE data

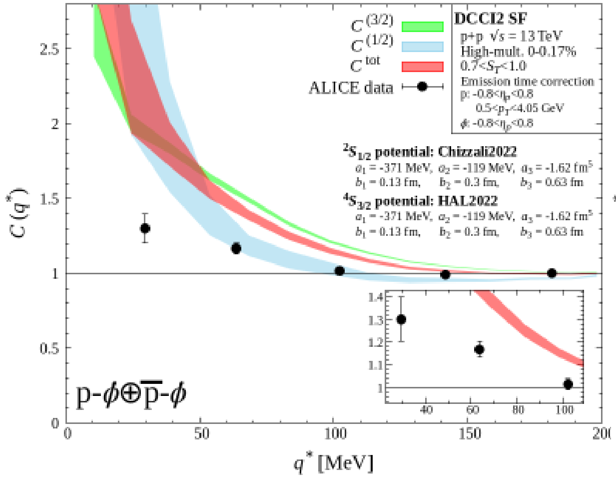

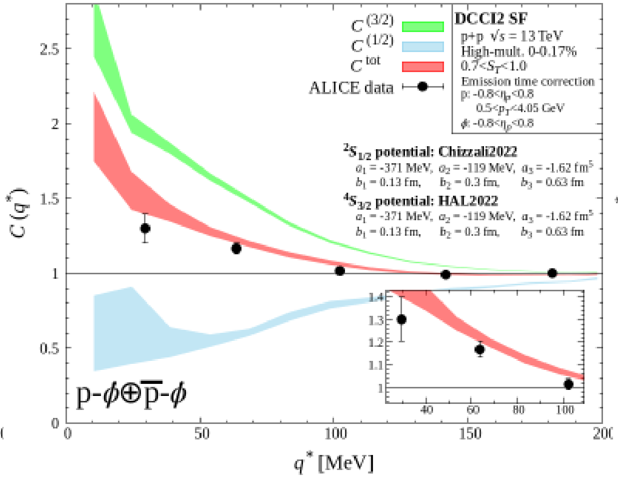

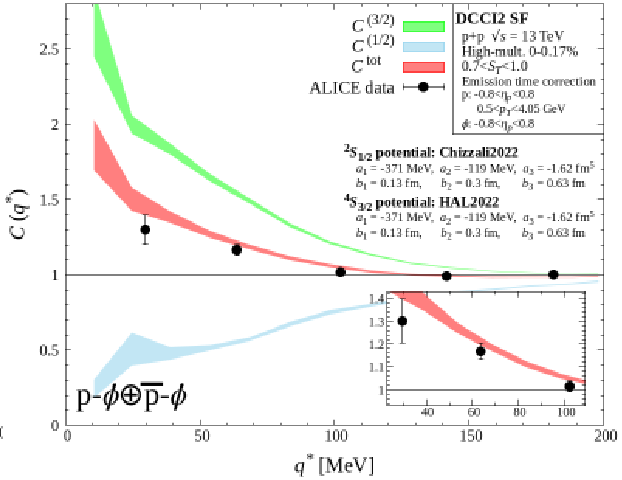

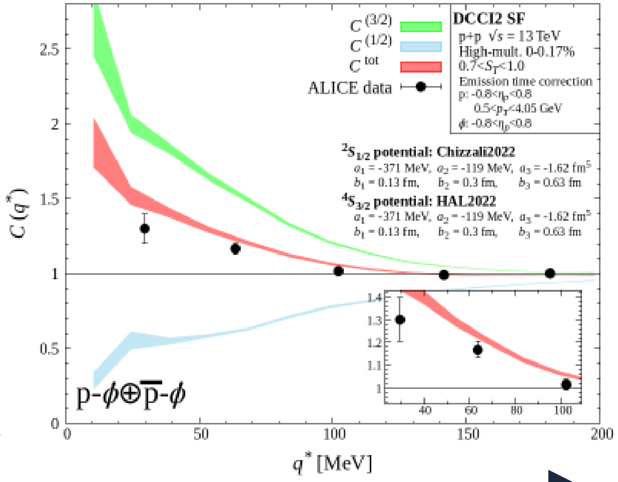

$\boldsymbol{\beta = 6}$	$\boldsymbol{\beta = 7}$	$\boldsymbol{\beta = 8}$	$\boldsymbol{\beta = 9}$
$a_0 = 4.54$ fm	$a_0 = 1.99$ fm	$a_0 = 1.23$ fm	$a_0 = 0.85$ fm
$E_B = 2.3$ MeV	$E_B = 13.3$ MeV	$E_B = 37.5$ MeV	$E_B = 93.1$ MeV

Overestimate | Agree within errors | Overestimate p–ϕ femtoscopy using SF from a dynamical model (DCCI2)

Effects of collision dynamics

Small but statistically significant

- Slightly larger source size due to hadronic rescatterings
- SF depends on the relative momentum due to e.g. collectivity

Constraint on interaction

Indication of a bound state in $^2S_{1/2}$ channel ($E_B \cong$ 10–70 MeV)

Importance of using SF that reflects collision dynamics
for precision hadron interaction study via femtoscopy

Backup

Koonin-Pratt formula

S. E. Koonin, PLB **70**, 43 (1977); S. Pratt, PRD **33**, 1314 (1986)

Assumptions

- **Chaotic source** ~ thermal equilibrium
- Same time approximation
- On-shell approximation
- **Closed system after emission** ~ In vacuum propagation

$$C(\boldsymbol{q},\boldsymbol{P}) = \frac{\int d^4x_a d^4x_b\, S_a(\boldsymbol{p}_a;x_a)S_b(\boldsymbol{p}_b;x_b)|\varphi(\boldsymbol{q};\boldsymbol{r})|^2}{\int d^4x_a\, S_a(\boldsymbol{p}_a;x_a)\int d^4x_b\, S_b(\boldsymbol{p}_b;x_b)}$$

Pair Rest Frame

Integrate out CM

$$C(\boldsymbol{q}) = \int d^3r\; S(\boldsymbol{q};\boldsymbol{r})\; |\varphi(\boldsymbol{q};\boldsymbol{r})|^2$$

Rewriting Koonin-Pratt formula

Spherical SF

$S(q;r)$

Only *s*-wave scattering

$$\varphi(\boldsymbol{q};\boldsymbol{r}) = \exp(i\boldsymbol{q}\cdot\boldsymbol{r}) - j_0(qr) + \varphi_0(q;r)$$

Plane-wave | **Plane-wave (*s*-wave)** | **w.f. (*s*-wave)**

$$C(\boldsymbol{q}) = \int d^3r\, S(\boldsymbol{q};\boldsymbol{r})\, |\varphi(\boldsymbol{q};\boldsymbol{r})|^2$$

$$= 1 + \int_0^\infty dr\, 4\pi r^2 S(q;r)\, \{|\varphi_0(q;r)|^2 - [j_0(qr)]^2\}$$

SF

w/ Jacobian

WF

Increase/Decrease of w.f. by **FSI**

Interpretation of correlation

Considering only *s*-wave scattering together with spherical SF

$$C(q) = 1 + \int_0^\infty dr \; 4\pi r^2 S(q;r) \; \{|\varphi_0(q;r)|^2 - [j_0(qr)]^2\}$$

SF
w/ Jacobian

Weight Function
Increase/Decrease in w.f. by interaction

Deviation of $C(q)$ from unity = **How much SF "picks up" WF**

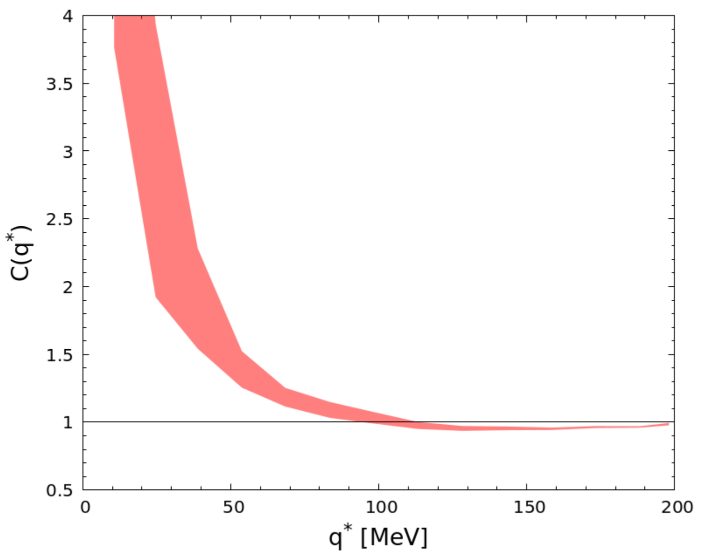

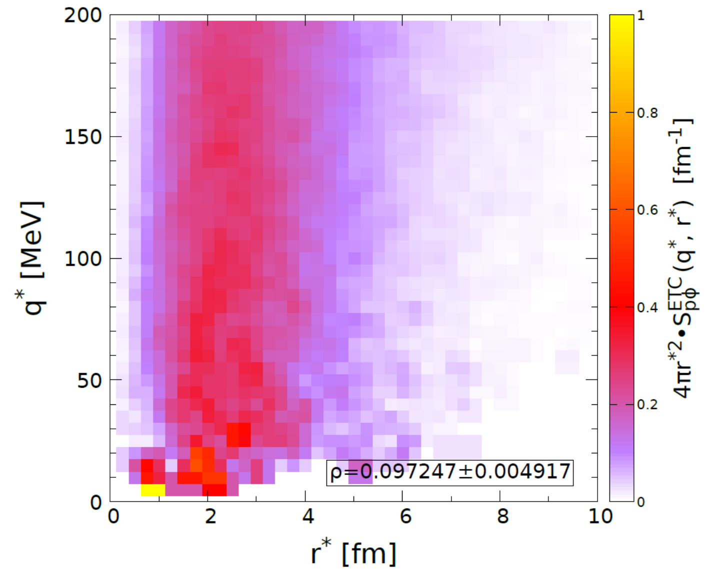

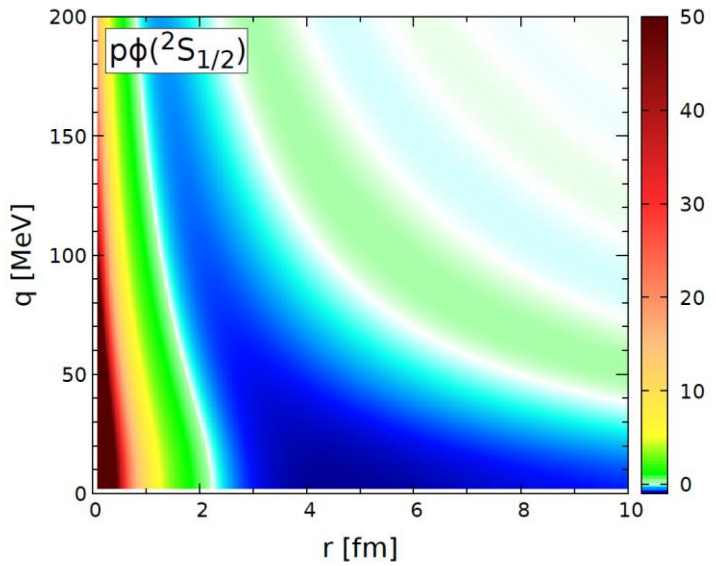

Interpretation of correlation

Considering only *s*-wave scattering together with spherical SF

$$C(q) = 1 + \int_0^\infty dr \; 4\pi r^2 S(q;r) \; \{|\varphi_0(q;r)|^2 - [j_0(qr)]^2\}$$

SF
w/ Jacobian

Weight Function
Increase/Decrease in w.f. by interaction

Deviation of $C(q)$ from unity = **How much SF "picks up" WF**

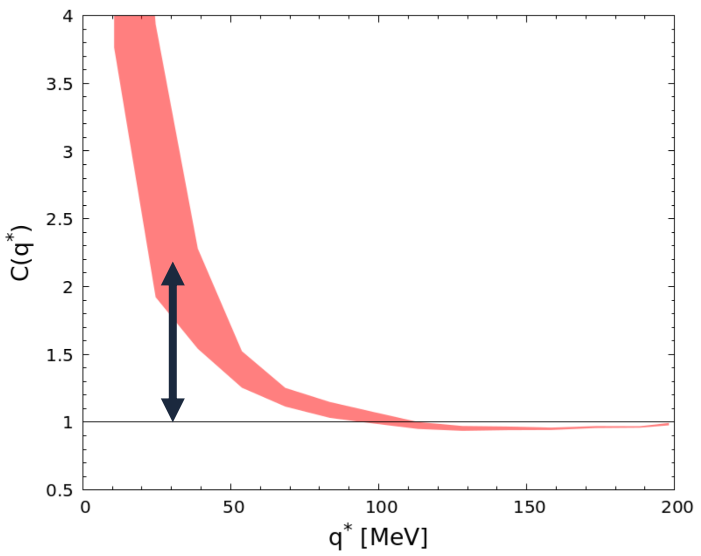

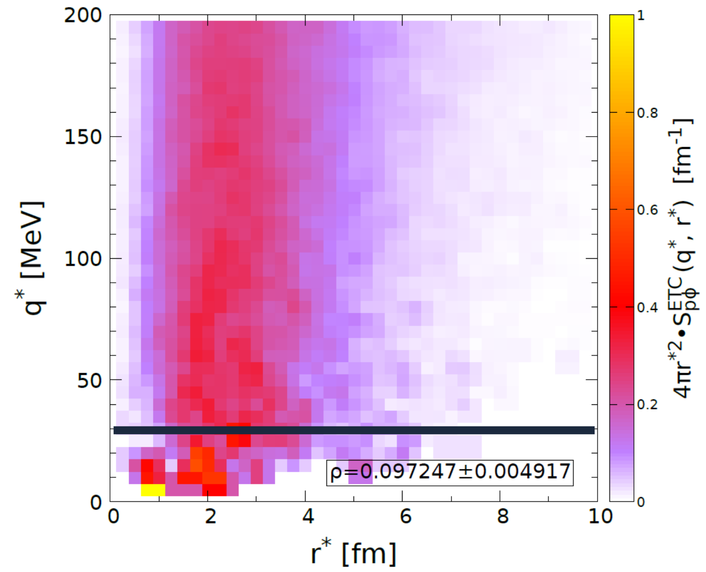

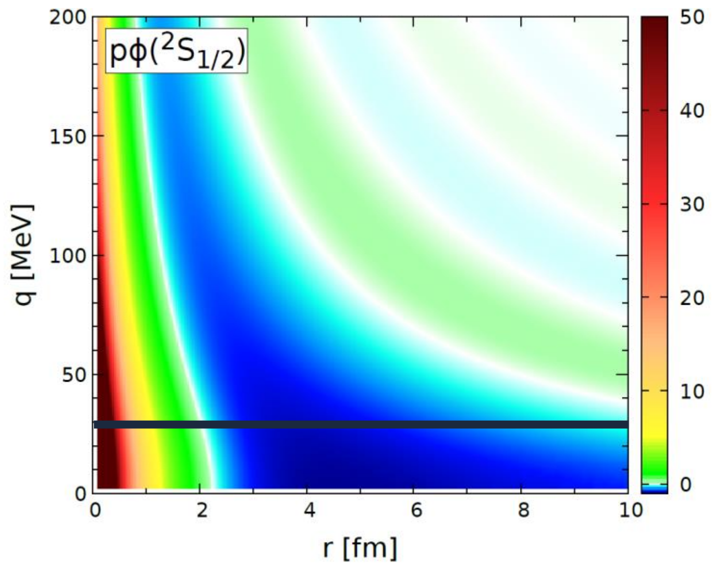

Interpretation of correlation

Considering only *s*-wave scattering together with spherical SF

$$C(q) = 1 + \int_0^\infty dr \; 4\pi r^2 S(q;r) \; \{|\varphi_0(q;r)|^2 - [j_0(qr)]^2\}$$

SF
w/ Jacobian

Weight Function
Increase/Decrease in w.f. by interaction

Deviation of $C(q)$ from unity = **How much SF "picks up" WF**

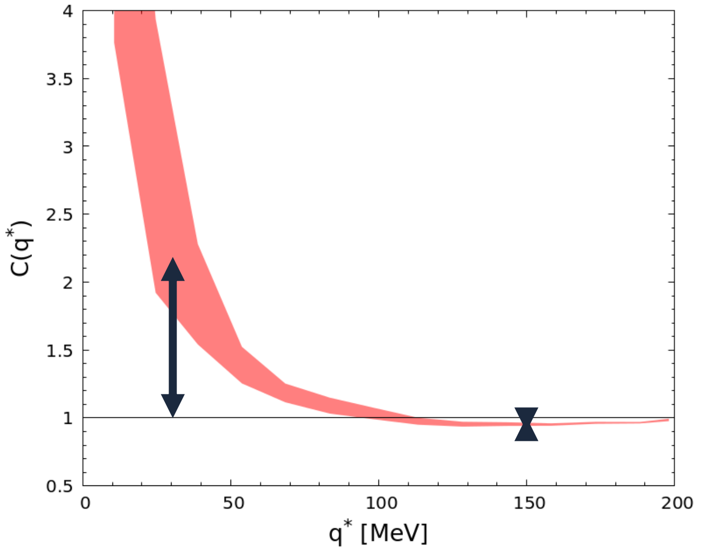

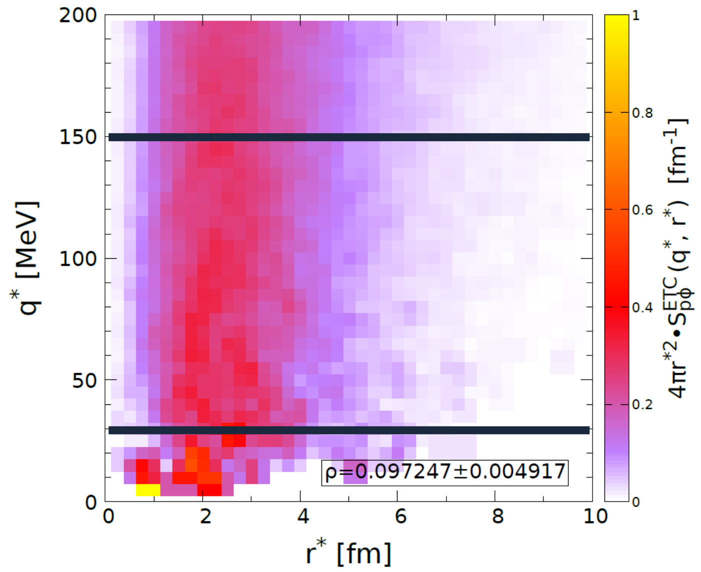

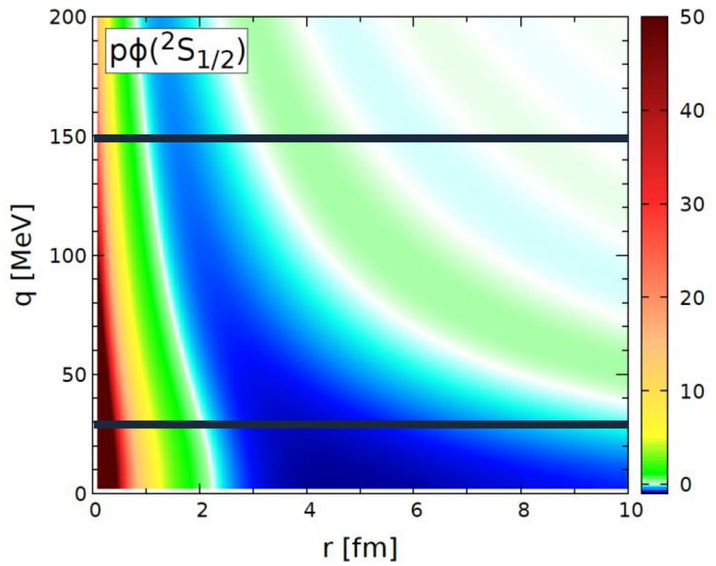

Lednický-Lyuboshits model

R. Lednický and V. L. Lyuboshits, Yad. Fiz. **35**, 1316 (1981)

$$C(q) = 1 + \int_0^\infty dr 4\pi r^2 S(q;r)\{|\varphi_0(q;r)|^2 - [j_0(qr)]^2\}$$

Assumptions

- **Gaussian**: $S(q;r) \approx S(r) \propto \exp\left(-\frac{r^2}{4r_0^2}\right)$
- **Asymptotic w.f.** (+ correction)

$$C(q) = 1 + \frac{|f_0(q)|^2}{2r_0^2} F_3\left(\frac{r_{\mathrm{eff}}}{r_0}\right) + \frac{2\mathrm{Re} f_0(q)}{\sqrt{\pi} r_0} F_1(2qr_0) - \frac{\mathrm{Im} f_0(q)}{r_0} F_2(2qr_0)$$

$F_1, \ldots, F_3$: Known functions, $f_0(q) = \frac{1}{q\cot\delta_0(q) - iq} \approx \frac{1}{-\frac{1}{a_0} + \frac{1}{2} r_{\mathrm{eff}} q^2 - iq}$

CF becomes a function of a_0, r_{eff}, and r_0

Relative w.f. w/ FSI

Focusing on low-q region with chaotic source and closed system assumptions
→ Steady-state Schrödinger eq. w/ central force

Partial-wave expansion

$$\varphi(\boldsymbol{q};\boldsymbol{r}) = \sum_{l=0}^{\infty}(2l+1)i^l\varphi_l(q;r)P_l(\cos\theta)$$

For each ${}^{2S+1}L_J$ channel,

$$\left[-\frac{1}{2\mu}\frac{d^2}{dr^2}+V(r)+\frac{1}{2\mu}\frac{l(l+1)}{r^2}\right]u_l(q;r)=\frac{q^2}{2\mu}u_l(q;r)$$

$u_l \coloneqq r\,\varphi_l$

Reduced mass:

$$\mu = \frac{m_a m_b}{m_a + m_b}$$

Core–corona ratio in p+p collisions

Y. Kanakubo, Y. Tachibana, and T. Hirano, PRC **105**, 024905 (2022)

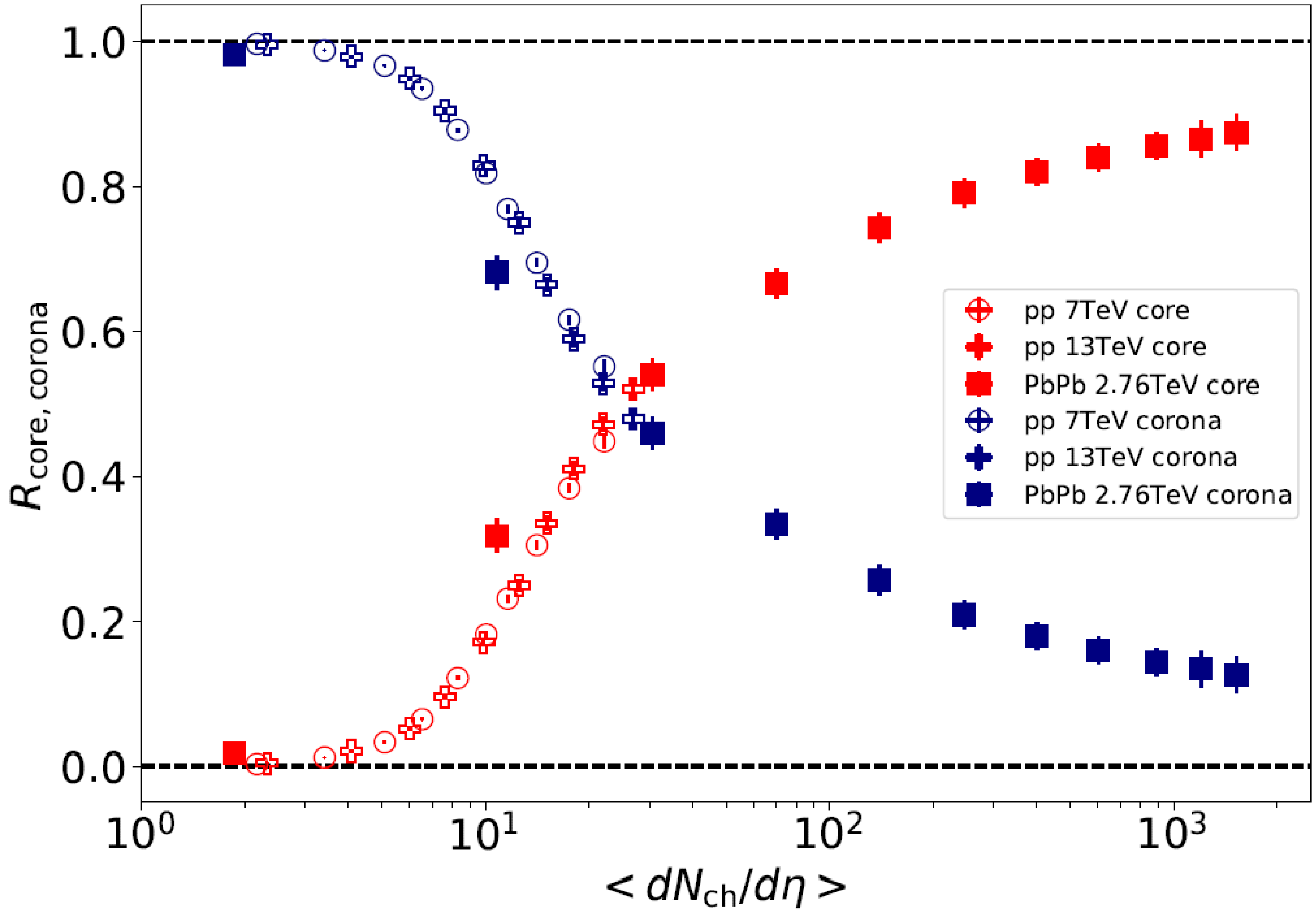

<u>According to DCCI2</u>

$R_{\mathrm{core}} \sim 0.5$

in high-multiplicity p+p collisions at $\sqrt{s} = 13$ TeV

Effects of collectivity

q-differential SF

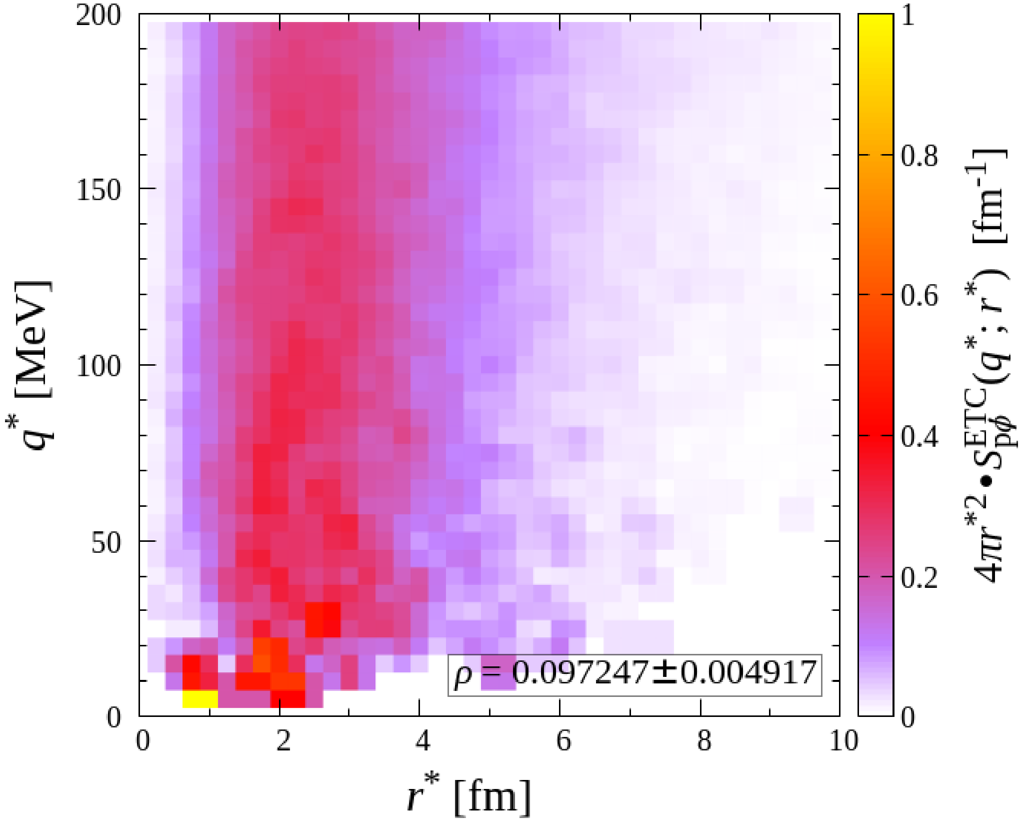

Positive q–r correlation

Collectivity of generated matter

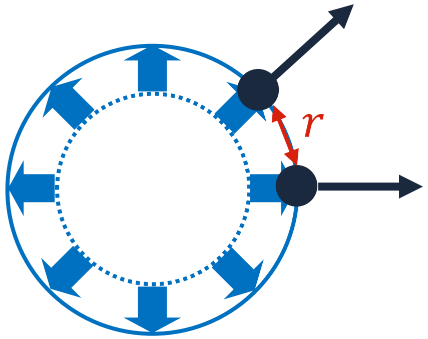

Close in position space

⇕

Close in momentum space

Spin-average

Relative w.f. = Weighted average of w.f. in each $^{2S+1}L_J$ channel

$$|\varphi|^2 = \sum_{\text{states}(S,L,J)} \omega_{(S,L,J)} \left|\varphi^{(S,L,J)}\right|^2$$

$$\omega_{(S,L,J)} = \frac{2S+1}{(2s_a+1)(2s_b+1)} \frac{2J+1}{(2L+1)(2S+1)}$$

KP formula

Spin-independent SF ← chaotic source

Spin-averaged CF

$$C^{\text{tot}}(\boldsymbol{q}) = \sum_{\text{states}(S,L,J)} \omega_{(S,L,J)}\, C^{(S,L,J)}(\boldsymbol{q})$$

⇒ Comparable w/ exp.

Weight Function: β-dependence

Weak — Attractive potential w/ a bound state — Strong

$\beta = 6$

$a_0 = 4.54$ fm

$E_B = 2.3$ MeV

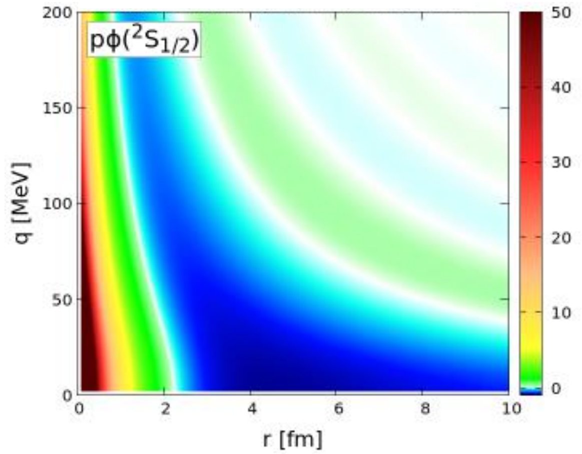

$\beta = 7$

$a_0 = 1.99$ fm

$E_B = 13.3$ MeV

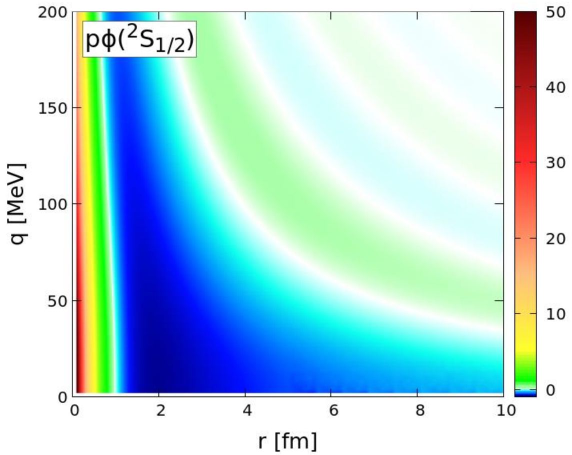

$\beta = 8$

$a_0 = 1.23$ fm

$E_B = 37.5$ MeV

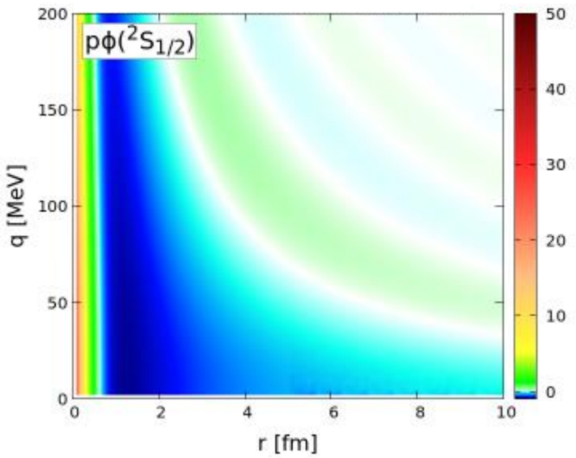

$\beta = 9$

$a_0 = 0.85$ fm

$E_B = 93.1$ MeV

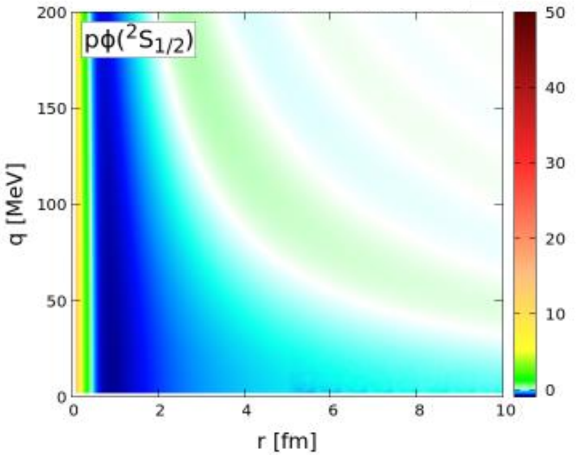

The negative valley moves towards the small r region

Effects of hadronic afterburner

Primordial core
Direct p and ϕ from core (hydro)

+ Decay → **Core w/ decay**: Effects of **feed-down**

+ Corona + Decay + Rescatterings → **Full**: Comparable with experiment)
Effects of feed-down & **rescatterings** (& corona)

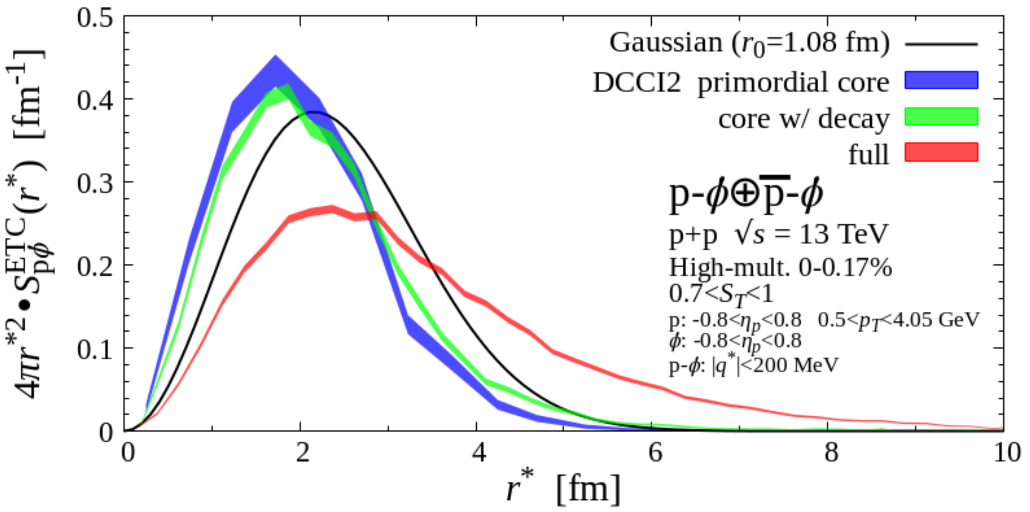

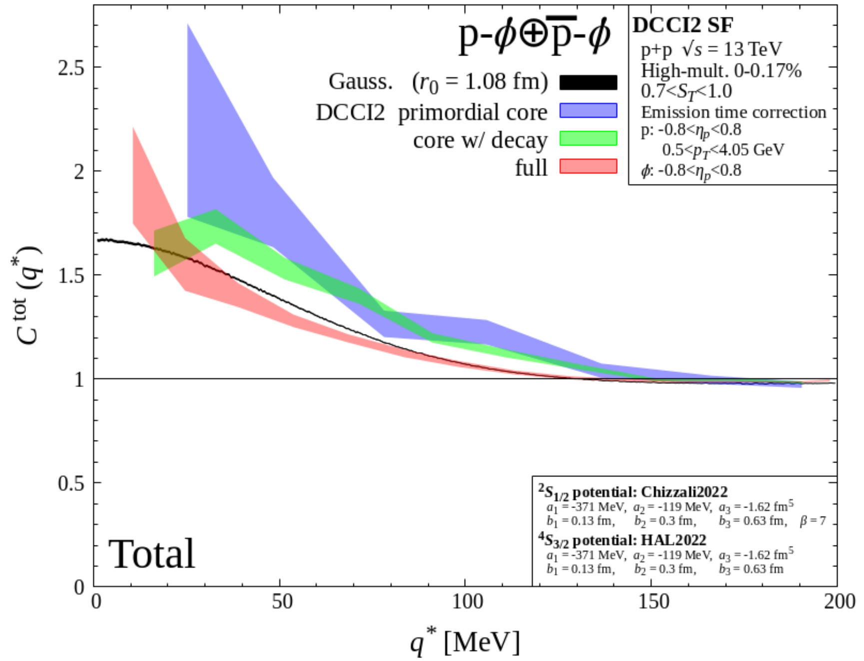

- ~Gaussian w/ smaller source size
- Decay → **A little long-tail**
- Rescatterings
  → **Long-tail and larger source size**

Larger effects of rescatterings than resonance decay on SF & CF

Emission Time Correction (ETC) at PRF

<u>Problem</u>

Dynamical model → **Emission time difference:** $S(\boldsymbol{q}; r^0 \neq 0, \boldsymbol{r})$

Violates **equal-time approximation** in KP formula

Free propagation until the other's emission

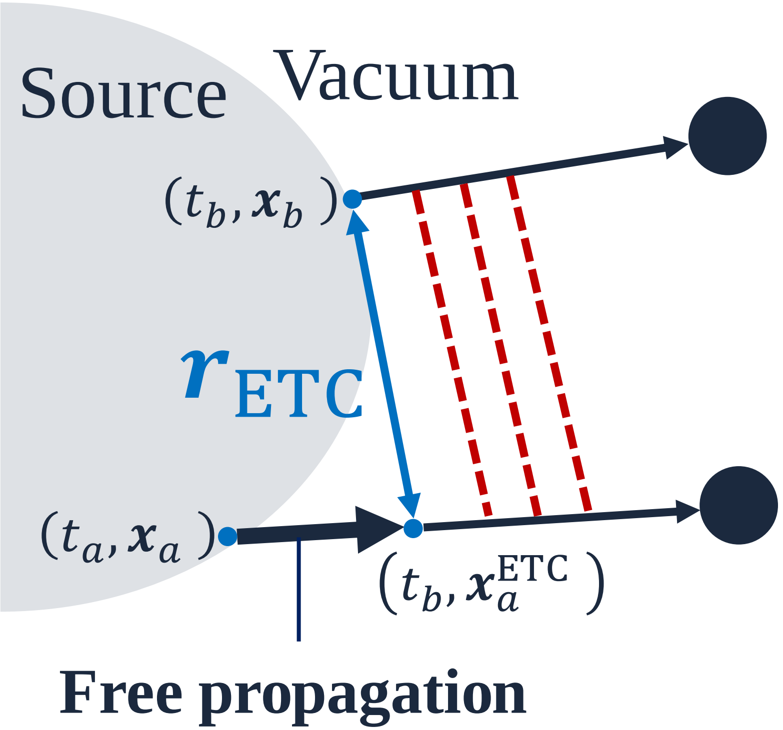

$$S(\boldsymbol{q}; r^0 \neq 0, \boldsymbol{r}) \xrightarrow{\text{ETC}} S^{\mathrm{ETC}}(\boldsymbol{q}; \boldsymbol{r}_{\mathrm{ETC}})\delta(r^0)$$

$$\boldsymbol{r}_{\mathrm{ETC}} = \boldsymbol{r} + \frac{\boldsymbol{p}_a}{E_a}(t_b - t_a)\theta(t_b - t_a) - \frac{\boldsymbol{p}_b}{E_b}(t_a - t_b)\theta(t_a - t_b)$$

Correction

Effects of ETC

Plots: w/ ETC,   Bands: w/o ETC

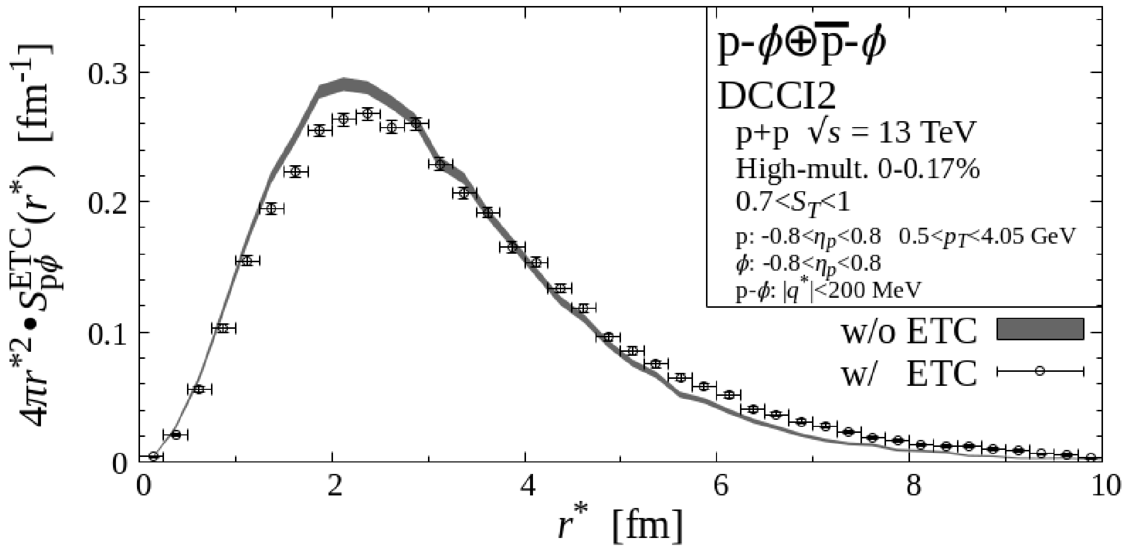

ETC slightly enlarge source size

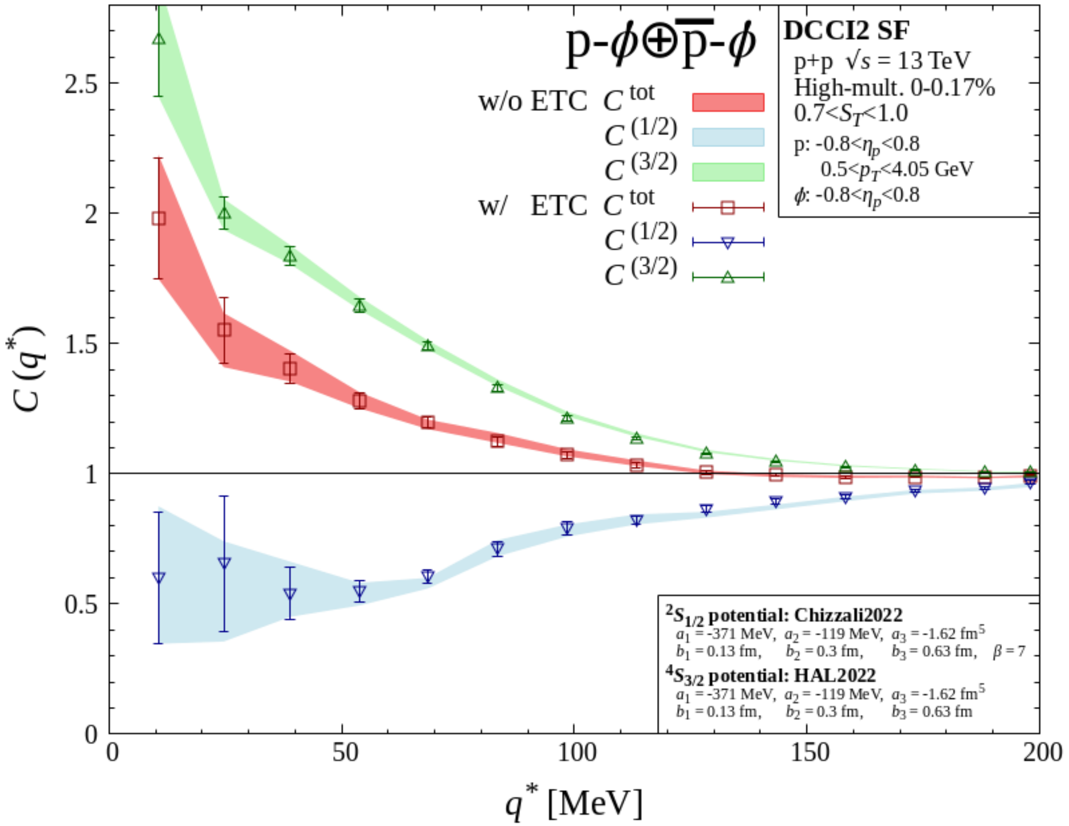

No statistically significant effects on CF in this particular case